



OPEN ACCESS

EDITED BY

Tianshou Ma,
Southwest Petroleum University, China

REVIEWED BY

Lucio Di Matteo,
University of Perugia, Italy
Roberto Greco,
University of Campania Luigi Vanvitelli,
Italy

*CORRESPONDENCE

Giacomo Pepe,
✉ giacomo.pepe@unige.it

RECEIVED 30 August 2023

ACCEPTED 13 November 2023

PUBLISHED 30 November 2023

CITATION

Fiorucci M, Pepe G, Marmoni GM, Pecci M, Di Martire D, Guerriero L, Bausilio G, Vitale E, Raso E, Raimondi L, Cevasco A, Calcaterra D and Scarascia Mugnozza G (2023), Long-term hydrological monitoring of soils in the terraced environment of Cinque Terre (north-western Italy). *Front. Earth Sci.* 11:1285669. doi: 10.3389/feart.2023.1285669

COPYRIGHT

© 2023 Fiorucci, Pepe, Marmoni, Pecci, Di Martire, Guerriero, Bausilio, Vitale, Raso, Raimondi, Cevasco, Calcaterra and Scarascia Mugnozza. This is an open-access article distributed under the terms of the [Creative Commons Attribution License \(CC BY\)](https://creativecommons.org/licenses/by/4.0/). The use, distribution or reproduction in other forums is permitted, provided the original author(s) and the copyright owner(s) are credited and that the original publication in this journal is cited, in accordance with accepted academic practice. No use, distribution or reproduction is permitted which does not comply with these terms.

Long-term hydrological monitoring of soils in the terraced environment of Cinque Terre (north-western Italy)

Matteo Fiorucci¹, Giacomo Pepe^{2*}, Gian Marco Marmoni³, Massimo Pecci⁴, Diego Di Martire⁵, Luigi Guerriero⁵, Giuseppe Bausilio⁵, Enza Vitale⁵, Emanuele Raso⁶, Luca Raimondi², Andrea Cevasco², Domenico Calcaterra⁵ and Gabriele Scarascia Mugnozza³

¹Department of Civil and Mechanical Engineering, University of Cassino and Southern Lazio, Cassino, Italy,

²Department of Earth, Environment and Life Sciences (DISTAV), University of Genova, Genova, Italy,

³Department of Earth Sciences, Sapienza University of Rome, Rome, Italy, ⁴Dipartimento per gli Affari Regionali e le Autonomie (DARA), Presidenza del Consiglio dei Ministri, Rome, Italy, ⁵Department of Earth, Environmental and Resource Sciences (DiSTAR), Federico II University of Naples, Complesso Universitario di Monte Sant'Angelo, Napoli, Italy, ⁶Cinque Terre National Park, La Spezia, Italy

Terraced landscapes represent one of the most widespread human-induced/man-made transformations of hilly-mountainous environments. Slope terracing produces peculiar morphologies along with unusual soil textures and stratigraphic features, which in turn strongly influence slope hydrology. The investigation of the hydrological features of terraced soils is of fundamental importance for understanding the hydrological dynamics occurring in these anthropogenic landscapes, especially during rainfall events. To this purpose, the availability of extensive field monitoring data series and of information on subsoil properties and structure is essential. In this study, multi-sensor hydrological data were acquired over a period longer than 2 years in the experimental site of Monterosso al Mare, in the Cinque Terre National Park (Liguria region, Italy), one of the most famous examples of terraced landscape worldwide. Monitoring data were coupled with accurate engineering-geological investigations to achieve the hydro-mechanical characterization of backfill soils and to investigate their hydrological response at both the seasonal and the single rainstorm scale. The results indicated that the coarse-grained, and anthropically remolded texture of the soils favors the rapid infiltration of rainwater, producing sharp changes in both soil volumetric water content and pore water pressure. Furthermore, the pattern of hydrological parameters showed seasonal trends outlined by alternating phases of slow drying and fast wetting. The study outcomes provide useful insights on the short and long-term evolution of hydrological factors operating in agricultural terraces. These findings represent a useful basis for a better understanding of the time-dependent processes that guide water circulation in terraced systems, which have a key role in controlling the occurrence of erosion and landslide processes.

KEYWORDS

agricultural terraces, Cinque Terre National Park, hydrological monitoring, soil hydrology, rainfall, terraced soils, shallow landslides

1 Introduction

Hilly and mountainous regions worldwide are notably prone to mass movements and erosion processes (Gutierrez et al., 1998; Dai and Lee, 2002; Guthrie and Evans, 2004; Crozier, 2006; Larsen, 2008; Harp et al., 2009; Coelho et al., 2011; Hungr et al., 2014). This primarily depends on the rugged and steep terrain morphology and on the fact that slopes typically are mantled by thin (from 0.5- to 3-m thick on average), loose and weathered soil/debris covers of various origin (e.g., eluvial-colluvial soils, pyroclastic soils, residual soils) (Dietrich et al., 1986). During intense rainstorms or rapid snowmelt, these materials become highly susceptible to landslides, mostly shallow failures (Fuchu et al., 1999; Cardinali et al., 2004; Guzzetti et al., 2004; Guadagno et al., 2005; Larsen and Wieczorek, 2006; Cevasco et al., 2013a; Schilirò et al., 2015; 2019; Giordan et al., 2017; Mandarino et al., 2021; Sepe et al., 2023). Failure initiation can be correlated to a wide range of destabilizing processes (Collins and Znidarcic, 2004; Lu and Godt, 2013; Bogaard and Greco, 2016), such as soil saturation due to the formation of a perched water table (Johnson and Sitar, 1990; Fannin and Jaakkola, 1999), slope-parallel or upward groundwater seepage (Iverson and Major, 1986; Crosta, 1998), matrix suction dissipation due to downward progression of a wetting front during rainwater infiltration (Rahardjo et al., 1995; Lacerda, 2007; Godt et al., 2008; Springman et al., 2013; Bordoni et al., 2015) and groundwater seepage mechanisms from fissures of the underlying bedrock (Freer et al., 2003; Guadagno et al., 2005; Cascini et al., 2008; Wooten et al., 2008).

Terraced slopes are one of the most widespread landscapes among hilly-mountainous environments, especially in regions where agricultural and rural activities have played, or still play, an important socio-economic role (Tarolli et al., 2014; Wei et al., 2016). Many of these anthropogenic landscapes are currently acknowledged as cultural heritage because of their historical and environmental value (Brandolini, 2017; Varotto et al., 2019). Terraces enable farmland activities in steep terrains, chiefly by modifying both slope morphology and hydrology (Arnáez et al., 2015; Moreno-de-las-Heras et al., 2019). The slope gradient reduction is obtained by cutting natural steep slopes to produce a step-like profile consisting of almost flat land strips limited by vertical or inclined risers. The excavated soil is employed as backfill material which can be sustained by dry-stone walls or by exploiting soil bioengineering solutions. Also, terracing works are coupled with artificial drainage systems (e.g., irrigation ditches, granular backfills placed directly behind walls). Accordingly, slope topography adjustment leads to a mitigation of both runoff and soil erosion processes, which in turn are accompanied by an increase in infiltration. This produces an increase in soil moisture content with both agricultural and ecological benefits (Stanchi et al., 2012). However, in case of intense rainfall, the progressive saturation of soils along with the development of critical regimes of pore-water pressures, can have negative consequences on slope stability (Crosta et al., 2003; Camera et al., 2012; 2014; Preti et al., 2018a). Moreover, backfill soils have been extensively remolded during slope terracing, producing unusual textural and stratigraphic features which can influence groundwater circulation (Gallart et al., 1997; Crosta et al., 2003; Cevasco et al., 2014; Preti et al., 2018a). The effects of hydrological processes coupled with the influence of other

factors, such as loss of efficiency and effectiveness of dry-stone wall and drainage works due to lack of maintenance, or land use conditions, can make terraced systems particularly vulnerable to rainfall-induced instability issues (Crosta et al., 2003; Lesschen et al., 2008; García-Ruiz and Lana-Renault, 2011; Brandolini et al., 2018; Cambi et al., 2021). The occurrence of mass movements along agricultural terraced slopes can have serious consequences in terms of economic loss, also in terms of risk scenarios for infrastructures, settlements and people (Galve et al., 2016; Agnoletti et al., 2019; Giordan et al., 2020).

To effectively address the complex hydrological dynamics occurring in terraced systems, it is essential to investigate the hydro-geotechnical properties of soils and to acquire the longest possible monitoring data series. To this purpose, experiences from case studies concerning local and peculiar slope contexts (e.g., climatic, geological, geomorphological, pedological, etc.) are very useful in providing valuable sources of data that can contribute to the advancement of knowledge. In literature, examples of long-term monitoring of unsaturated terraced soils properties are rarely reported (Camera et al., 2012; Preti et al., 2018b; Nunes et al., 2018; Pijl et al., 2020; Schilirò et al., 2023).

This paper presents the results of more than 2 years of continuous monitoring of soil hydrological properties in a terraced site in the Cinque Terre National Park (north-western Italy). This strip of coastal land has been a UNESCO World Heritage Site since 1997 due to the environmental, historical and cultural significance of its human-modified landscape characterized by agricultural terraced slopes (Brandolini, 2017), which cover a large percentage (41%) of the entire park surface (38 km²) (Raso et al., 2021). The main goals of the present work are i) to provide the hydro-mechanical characterization of soils, showing coarse-grained and well-graded textures, which were anthropically reworked as backfill of agricultural terraces and ii) to investigate the hydrological response of terraced soils during either seasonal periods (i.e., following dry and wet phases) and intense rainstorms. The outcomes of this study are expected to provide a useful contribution to improve knowledge on hydrological processes developing in agricultural terraces.

2 General setting of the study area and of the monitoring site

The study area is located in the easternmost part of the Liguria region (north-western Italy, La Spezia Province), within the small coastal catchment (3.2 km²) of the Pastanelli stream, which entirely flows within the municipality of Monterosso al Mare towards the Ligurian Sea (Figure 1A).

From a geological point of view, this coastal sector of Liguria corresponds to a segment of the Northern Apennine (Abbate et al., 2005), and it shows typical hilly-mountainous morphologies (Brandolini, 2017; Raso et al., 2021). Since 1999, this area has been included within the Cinque Terre National Park (Figure 1A), which encloses land portions belonging to five municipalities (i.e., Monterosso al Mare, Vernazza, Riomaggiore, Levanto and La Spezia). Within the Pastanelli catchment, the bedrock is primarily characterized by sandstone-claystone turbiditic successions (Macigno Fm., Tuscan Nappe, Upper

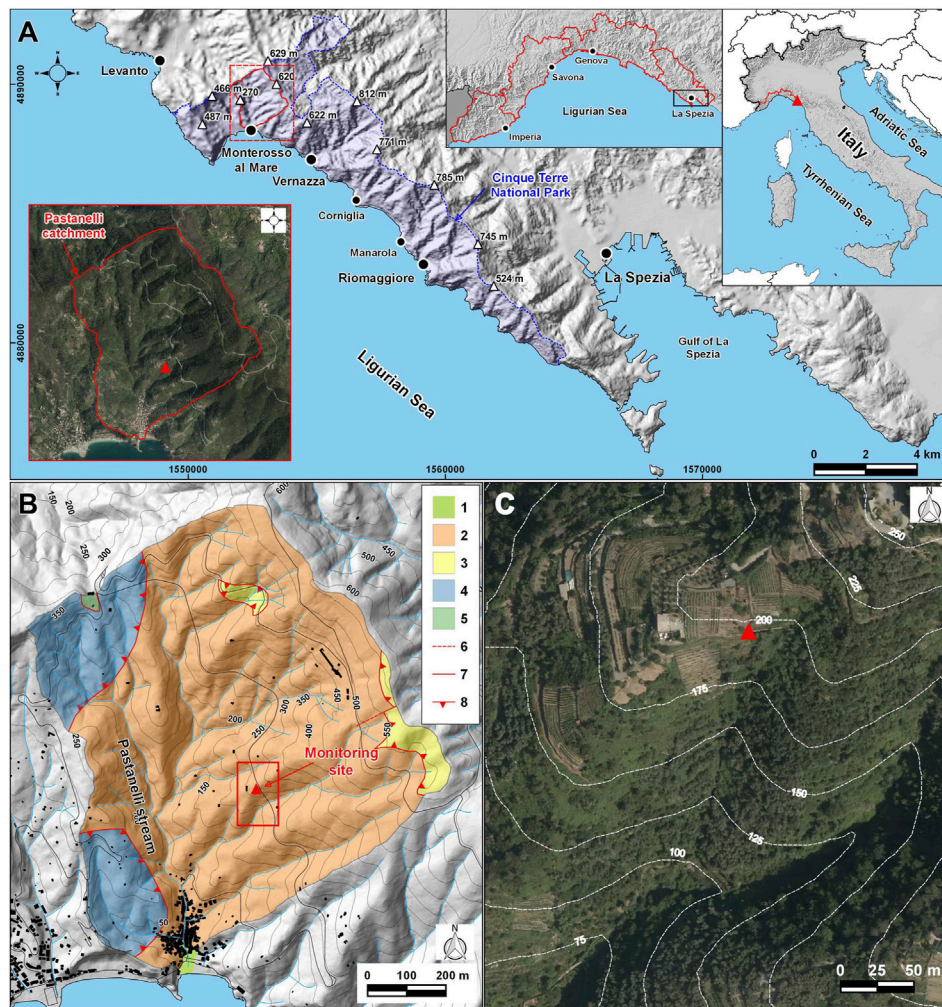


FIGURE 1

(A) Location of the study area and of the monitoring site (base maps derived from a 20 m cell-size DEM, source: Istituto Superiore per la Protezione e la Ricerca Ambientale; orthophoto was taken by Regione Liguria in 2016). (B) Geologic map of the Pastanelli catchment: 1, Quaternary deposits; 2, Macigno Fm.; 3, Canetolo Shales and Limestones Fm.; 4, Monte Veri Shales Fm.; 5, serpentinites; 6, tectonic contact; 7, fault; 8, thrust (base maps derived from a 5 m cell-size DEM, source: Geoportale Regione Liguria). (C) Detailed view of the slope section where the monitoring station was installed (orthophoto was taken by Regione Liguria in 2016).

Oligocene) and secondarily by sedimentary bodies mostly consisting of assemblages of shales and breccias (Monte Veri Shales Fm., External Ligurides, Campanian) (Figure 1B). Small outcrops mainly consisting of pelitic, calcareous and silty-arenaceous rocks (Canetolo Shales and Limestones Fm., Sub-ligurian Domain, Paleogene) and of ophiolitic shreds made up of serpentinites (Jurassic - Internal Ligurides Domain, Jurassic) complete the geology of the basin (Abbate et al., 2005). Geomorphologically, the catchment is characterized by a high relief energy, highlighted by steep slopes carved by a tight system of V-shaped valleys that are drained by steep and straight creeks (Raso et al., 2021). Slopes are mantled by shallow soils (typically <3 m-thick) deriving from the weathering of bedrock and from both gravity- and runoff-related processes (i.e., eluvial-colluvial deposits). Slope deposits have a prevalent sandy-gravel or gravelly-sand texture (Cevasco et al., 2013a; 2014; Scopesi et al., 2020). Over the centuries, slope materials have been largely reworked by humans across the basin

due to agricultural terracing (Terranova et al., 2002; Brandolini, 2017; Pepe et al., 2019).

The monitoring site is located on the right side of a small secondary valley drained by a left tributary of the Pastanelli stream, in close proximity to the slope ridge (Figure 1C). Such slope shows the typical morphology and land use setting of the whole Cinque Terre area (Raso et al., 2021). It is a south-facing terraced slope which regularly descends towards the valley bottom with topographic gradients ranging between 20° and 40°; to the east, the slope is bordered by a small and straight stream of first order. The slope elevation varies between 205 and 90 m a.s.l., while the monitoring site is located at approximately 195–200 m a.s.l. The monitored site has an average gradient of approximately 27° along the longitudinal profile and it shows a step-like morphology connected to the presence of agricultural terraces sustained by 1.5–2.0 m high dry-stone walls. Terraces are cultivated with vineyards and orchards. Below the investigated site, land use is

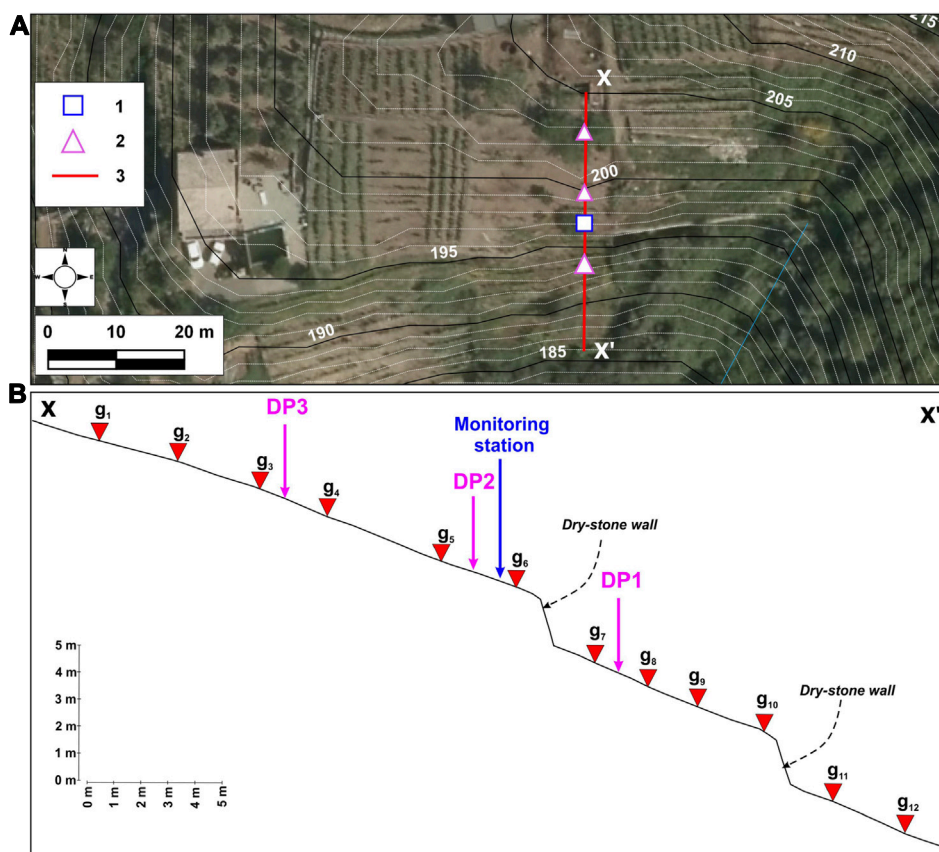


FIGURE 2

(A) Location of geotechnical and geophysical field investigations (orthophoto was taken by Regione Liguria in 2016): 1, monitoring station; 2, dynamic probing test (DPM); 3, seismic refraction survey. (B) Detailed view of dynamic probing test location and of seismic array.

mainly characterized by abandoned terraces covered by both shrubs and forest tree species. Along this part of the slope, some morphological fingerprints (e.g., crowns, runout trajectories) of shallow landslides and debris flows triggered during the 25 October 2011 rainstorm are still visible (Cevasco et al., 2015a; Schilirò et al., 2018; Pepe et al., 2020). Around the monitored site, sparse bedrock outcrops, made up of alternation of thin bedded (5–20 cm) fine-grained sandstones and siltstones belonging to the Riomaggiore Banded Sandstones lithofacies (Macigno Fm), are present; the outcropping rock masses are both heavily fractured and weathered.

According to the Köppen climate classification (Köppen, 1884), the area of the Cinque Terre has a typical Mediterranean climate, indexed as Cs. This climate is characterized by dry summers with a high probability of drought and rainy winters with mild temperatures. Referring to the nearest weather station, installed just west of the Monterosso al Mare urban center, and to a data series available from 2005 to 2022 (Regione Liguria, 2022), the average annual temperature is 16°C, while the coldest month is January (9°C) and the hottest one is July (25°C). The average annual cumulated rainfall is 1,075 mm; the maximum average monthly rainfall values are in October and November (141 and 137 mm, respectively), whereas the minimum ones are in July and June (40 and 49 mm, respectively). During the autumn season, prolonged hot and dry periods can be followed by intense rainfall episodes that are often a

source of significant ground effects (Cevasco et al., 2015a; Galanti et al., 2018; Raso et al., 2019).

3 Materials and methods

3.1 Field investigations

A combination of *in-situ* geotechnical and geophysical investigations was carried out to define a 2-D engineering-geological ground model across the monitoring site. Field tests were executed along an alignment, oriented roughly parallel to the local dip direction of the slope, whose trace passes through the monitoring station (Figure 2A).

Three dynamic probing (DP) tests were performed to detect the bedrock depth and to investigate the degree of compaction of soils. Two DP tests were executed close to the upstream and downstream ends of the alignment, while one was carried out close to the installed hydro-geotechnical monitoring instruments (Figure 2). A medium dynamic penetrometer (DPM) (Stefanoff et al., 1988) was used, because of easily transportable on steep terraced slopes (D'Amato Avanzi et al., 2013); this equipment works with a 30 kg hammer mass dropping from a 20 cm height to drive steel rods and a conical tip (diameter 35.7 mm, tip angle 90°, cross section 10 cm²) through the ground. The number of blows required to advance the steel

conical tip through the soil for each rod length of 10 cm (N_{10}) was registered. The test ended when $N_{10} \geq 50$, assuming this condition as indicative of bedrock occurrence. In order to evaluate the state of soils, N_{10} was normalized to the number of blows referred to the Standard Penetration Test (N_{SPT}) by means of a correlation factor taking into account the ratio between the specific energies per blow for the two test types (i.e., $N_{SPT} = \delta \cdot N_{10}$ with $\delta = 0.73$) (Odebrecht et al., 2005; D'Amato Avanzi et al., 2013). The empirical correlation between N_{SPT} and the relative density (D_R) proposed by Gibbs and Holtz (1957) was then used.

The seismic refraction survey consisted of one tomographic profile, which was centered with respect to the monitoring station. The DPM tests were carried out along the same alignment as the seismic refraction survey. P-wave seismic data were acquired with twelve geophones measuring ground movements with a natural frequency of 4.5–10 Hz (Figure 2). Geophones were connected to a multi-channel seismograph with digital data acquisition and with a sampling frequency of 5,000 Hz; an acquisition time window of 0.25 s was used. An 8 kg sledge-hammer hitting a steel plate was employed as a seismic source of 10 shots regularly distributed along the selected seismic array. The field campaign also included five soil density measurements using the sand cone method (ASTM Committee on Standards, 2007), executed around the monitoring station. Eventually, undisturbed soil samples were collected for laboratory geotechnical investigations.

3.2 Geotechnical laboratory testing

Three disturbed soil samples (namely, A, B and C), collected near the monitoring station and at a surficial depth equal for all three samples, were characterized by means of mineralogical and physical analyses. The mineralogical composition was investigated by means of X-Ray diffraction analysis (XRD) performed on randomly oriented powder using Malvern Panalytical X'Pert Pro modular diffractometer.

Physical characterization tests of the soil consisted of determining particle size distribution, specific gravity and plasticity characteristics (i.e., Atterberg limits). Particle size distribution curves were obtained from dry sieving and hydrometer sedimentation tests according to ASTM D 422–63 (ASTM Committee on Standards, 2000). Specific weight was determined following the ASTM D 854–92e1 (ASTM Committee on Standards, 1998). Liquid and plastic limits were measured according to standard methods described by ASTM D4318-10 (ASTM Committee on Standards, 2010). The difference between the liquid and plastic limits was defined as the plasticity index ($PI = w_L - w_p$). The initial water content of soil samples was measured by means of ASTM D 4959-00 (ASTM Committee on Standards, 2000). Measurements of the organic matter (OM) were performed following the procedure stated by ASTM D2974 (ASTM Committee on Standards, 2014). The sample was initially weighed after 24 h in an oven at 105°C. The time of exposure of the sample to the 440°C temperature in the muffle furnace lasted 24 h. The sample was then placed in a desiccator and then weighed after cooling.

Mechanical behavior of soil was investigated by means of direct shear tests and one-dimensional compression tests performed on saturated reconstituted samples. The shear box apparatus adopted is a standard one, the shear force being developed by an electric motor driving, providing a variable speed control ranging from 5×10^{-4} to

2 mm/min. All direct shear tests were performed at a 0.5 mm/min displacement rate. Micrometer dial gauges with an accuracy of 0.001 and 0.01 mm were used to measure vertical and horizontal displacements, respectively. Tests were performed at stress levels of 100, 200 and 300 kPa. One dimensional loading was performed in standard oedometer cells, where vertical stress was conventionally applied in successive steps ($\Delta\sigma_v/\sigma_v = 1$) within the stress interval $10 \div 2,500$ kPa. Micrometer dial gauges with an accuracy of 0.001 mm were used to measure vertical displacements.

3.3 Installed monitoring network

As of 2018, field monitoring was conducted according to two different sensor configurations. The first configuration was active, net of outages, until the end of 2020 and the multi-parametric monitoring system was composed of: a weather station equipped with thermo-hygrometer and rain gauge, four tensiometers (coded by T1 to T4) for the measurement of soil water pressure within the range -85 kPa/+100 kPa (model T4e, UMS, München, Germany), four soil moisture sensors (coded by W1 to W4) for the measurement of soil volumetric water content (model ECH2O EC-5, Meter group, Pullman, WA) and one combined sensor (coded W5) for the estimation of soil volumetric water content and temperature (model ECH2O 5TM, Meter group, Pullman, WA). The depth of installation of tensiometers and soil moisture sensors was 50 cm and 100 cm b.g.l. to evaluate the spatial variability of hydraulic conditions over time (Figure 3A for more details). The monitored data were recorded by a Campbell Scientific CR1000 datalogger, set with a sampling rate of 5 min, powered by a solar panel and lithium backup batteries, which guarantees its functioning even during episodes of severe weather. The first configuration was updated in October 2022 with the installation of new sensors and replacing those that no longer worked. This second configuration (Figure 3B) is now composed of: a weather station equipped with an air thermometer, a hygrometer, a rain gauge, an anemometer and a wind vane, four soil moisture sensors (coded by SM1 to SM4) for the measurement of soil volumetric water content (model ECH2O EC-5, Meter group, Pullman, WA), four combined sensors (coded by WP1/WT1 to WP4/WT4) for the monitoring of soil water potential and temperature (model TEROS 21, Meter group, Pullman, WA) and one combined sensor (coded SM5) for the measurement of soil volumetric water content and temperature (model ECH2O 5TM, Meter group, Pullman, WA). In this second case, the soil water content sensors and the soil water potential sensors were installed at only two points, namely, at 50 cm and 80 cm b.g.l., to reconstruct a log with the depth (Figure 3B). The recorded data are automatically transmitted to a remote server every 12 h thanks to a GSM/GPRS connection. The storage platform can be reached by cloud access from the web, allowing the complete management of the monitored data series.

3.4 Monitoring data analysis

Data from the field monitoring system were managed following an Observation-Based Approach (Fiorucci et al., 2020), which is based on the research of objective cause-to-effect relations among environmental stressors and hydraulic soil responses. For a correct

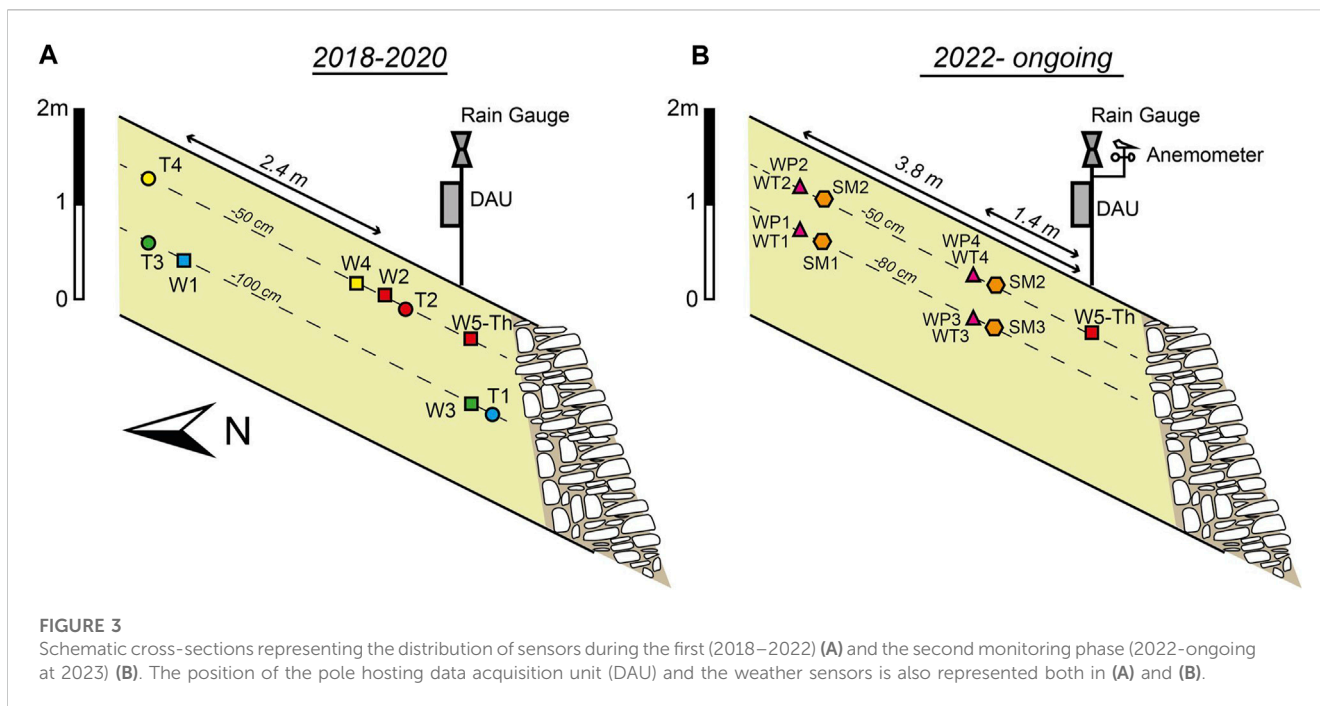


FIGURE 3 Schematic cross-sections representing the distribution of sensors during the first (2018–2022) (A) and the second monitoring phase (2022–ongoing at 2023) (B). The position of the pole hosting data acquisition unit (DAU) and the weather sensors is also represented both in (A) and (B).

use of the OBA data analysis approach, it is necessary to have a well-constrained engineering-geological and evolutionary model of the slope. For this reason, the case study presented here lends itself well to its application. In this specific case, continuous and discontinuous data were recorded. The first category includes temperature, soil water pressure and soil water content, which are parameters recorded over time without null values. The second category is represented by data referring to transient and/or impulsive actions with a certain intensity in a certain time, like rainfall: the latter is a trigger in slope instabilities at the catchment scale. The datasets reconstructed in this way provided the time series of environmental parameters and hydraulic soil conditions, which were analyzed thanks to the comparison made on synoptic tables.

By coupling the pore water pressure and water content data monitored in the field, it was possible to reconstruct the soil's average characteristic water retention curves (SWRCs) for the two depths investigated. The point-by-point SWRCs obtained from soil data were fitted using logarithmic correlations and then compared with those obtained according to the equations provided by van Genuchten (1980) (Eq. 1) and by Kosugi (1999) (Eq. 2) using the SWRC fitting proposed by Seki et al. (2023). From these last equations, it was possible to predict the hydraulic parameters of the soil, as follows:

$$S_e = \left[\frac{1}{1 + (\alpha h)^n} \right]^m; m = \left(1 - \frac{1}{n} \right) \tag{1}$$

where S_e represents the effective saturation, h is the pressure head while α and n are fitting parameters (van Genuchten, 1980);

$$S_e = Q \left[\ln \left(\frac{h}{h_m} \right) / \sigma \right]; Q(x) = \text{erfc} \left(\frac{x}{\sqrt{2}} \right) / 2 \tag{2}$$

where Q denotes the complementary normal distribution function, h_m is the pressure head related to the median soil pore radius while σ

is a dimensionless parameter (Kosugi, 1999). In this way, the effective saturation (S_e) is expressed as follows:

$$S_e = \frac{(\theta - \theta_r)}{(\theta_s - \theta_r)} \tag{3}$$

where θ is the volumetric water content, and θ_s and θ_r are the saturated and residual moisture contents, respectively. Hence, the volumetric water content can be written as follows:

$$\theta = \theta_r + (\theta_s - \theta_r) S_e \tag{4}$$

4 Results

4.1 Test site engineering-geological characterization

The results of DPM tests pointed out that the reworked eluvial-colluvial deposits show small thickness along the monitored slope section: the bedrock level was approximately detected between 1.0 and 1.7 m b.g.l (Figure 4A). From the N_{10} -depth profiles (Figure 4A), it can be noted a quite homogeneous state of soils, since they resulted in values of D_R lower than 20%, namely, from loose to very loose. In some localized cases, especially in the proximity of soil levels directly overlying the bedrock (e.g., tests DP1 and DP2), the N_{10} -depth profiles revealed slightly more compact horizons (D_R around 30%). However, these profiles show an irregular trend, likely correlated to the presence of pebbles. These results are consistent with those of the geophysical surveys, which revealed a progressive increase in density with depth in the investigated site (Figure 4B). Specifically, reworked eluvial-colluvial soils exhibit P-wave velocities lower than 600 m/s, while across the underlying

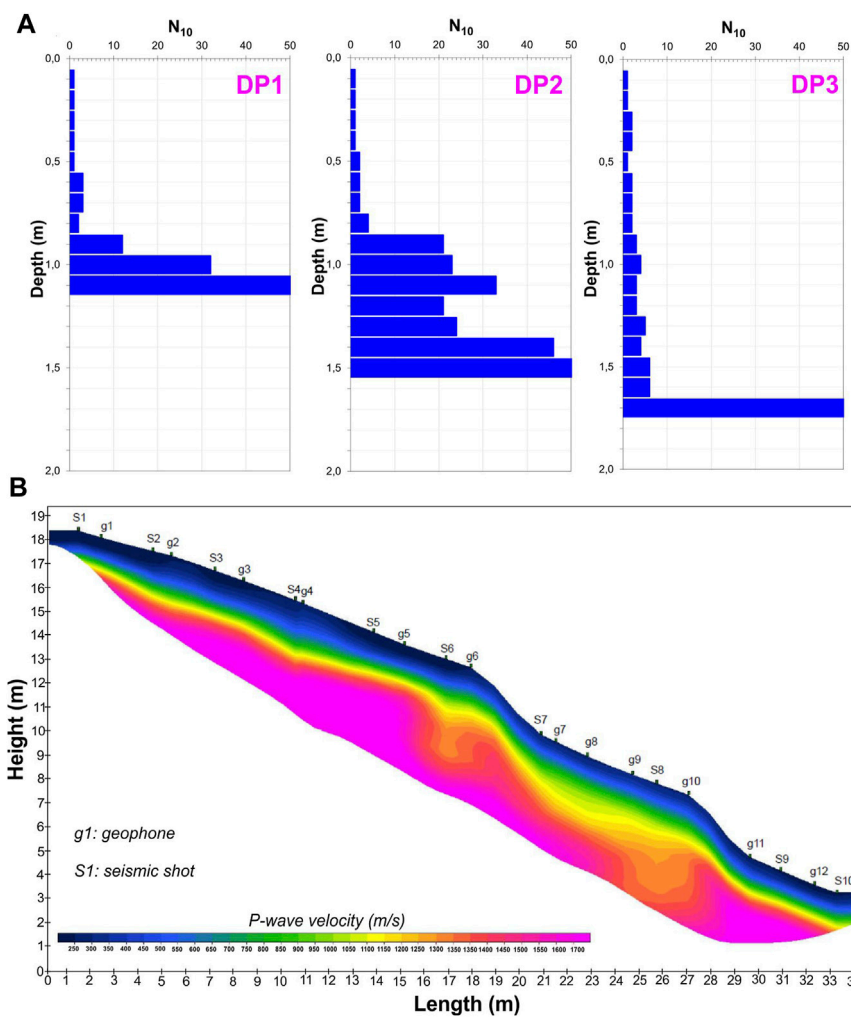


FIGURE 4
In-situ investigation results: (A) dynamic penetration profiles (N_{10} vs. depth); (B) P-wave seismic refraction tomography profile.

bedrock V_p ranges from 600 up to 1,700 m/s, depending on both the degree of fracturing and weathering.

Based on the combination of direct and indirect field investigations, an engineering-geological 2-D model of the selected slope segment was defined, which consists of three main horizons (Figure 5): 1) reworked eluvial-colluvial soils ($V_p < 600$ m/s); 2) weathered and fractured bedrock ($600 < V_p < 1,100$ m/s) and 3) fresh and un-weathered bedrock ($1,100 < V_p < 1,700$ m/s).

From the outcomes of the *in-situ* soil density measurements, the investigated soils show the following average physical properties: natural unit weight of 14.6 ± 1.05 kN/m³, dry unit weight of 13.2 ± 0.97 kN/m³, and a computed total porosity of 0.49 ± 0.05 .

4.2 Geotechnical soil characterization

As results from XRD analysis, the soil samples are composed of vermiculite, quartz and muscovite with small amounts of albite, with an average percentage of organic matter equal to 5,40%. The specific gravity of particles ranges from 2.5 to 2.7 g/cm³ while the initial

water content is about 11%. Grain size distributions of the soil samples are reported in Figure 6A. The percentage by weight of fine grains (clay and silt) is larger for samples A and B compared to sample C. Sand fraction ranges from 24,7% to 28,5%, whereas gravel content is about 50% for samples A and B and 60,2% for sample C. Laboratory determination of plasticity characteristics of soil samples showed a range of 27%–30% and 35%–41% for plastic limit (w_p) and liquid limit (w_l) respectively. Plasticity Index (PI) varies between 8% and 13%, showing a low plasticity of the tested soil samples. Based on the unified soil classification system (USCS), the fine-grained soil fraction is classified as inorganic silts with low to medium plasticity (ML) and organic silts and clays of low plasticity (OL) (Figure 6B). Therefore, based on these outcomes, the soil samples were classified as silty gravels (GM) according to the USCS scheme.

Results of direct shear tests are reported in Figures 7A, B. Under applied confining stresses of 100, 200 and 300 kPa respectively, soil samples show a ductile and contractile behavior. The values of shear stresses (τ) at the end-of-test are plotted in Figure 7C in a conventional Mohr-Coulomb plot, as a function of vertical effective stress (σ'_v). The linear failure envelope used to define

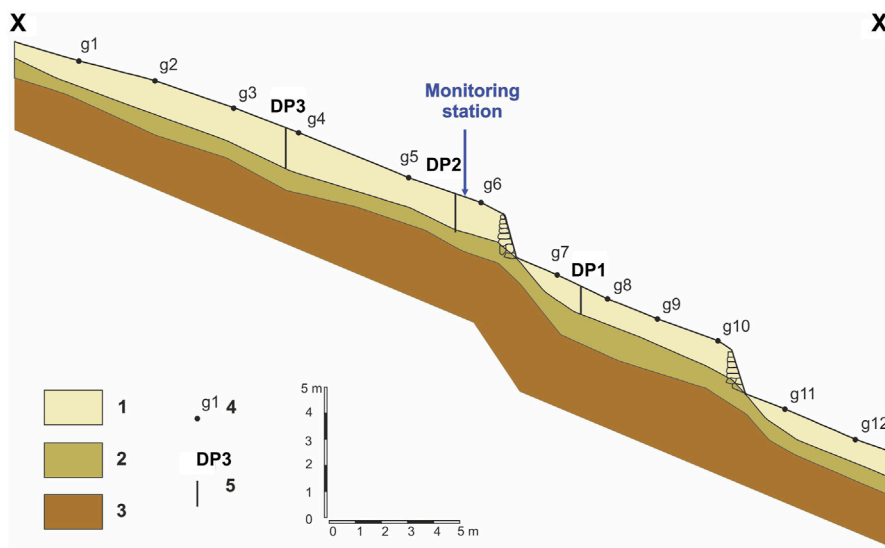
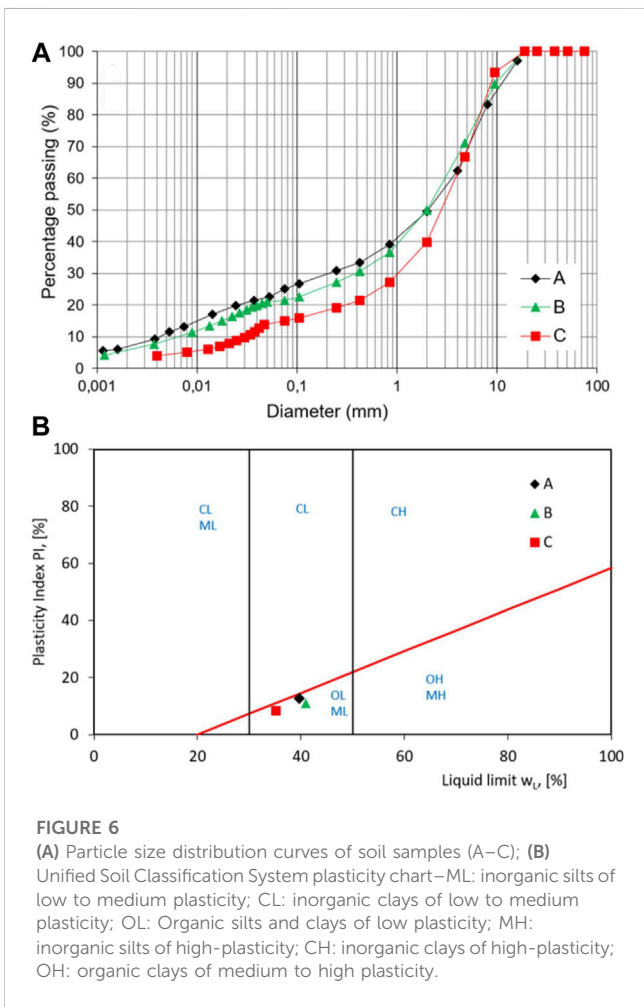


FIGURE 5 Engineering-geological cross section across the monitored slope section: 1. Reworked eluvial-colluvial deposits; 2. Weathered and fractured bedrock; 3. Fresh and fractured bedrock; 4. geophone; 5. dynamic probing test.

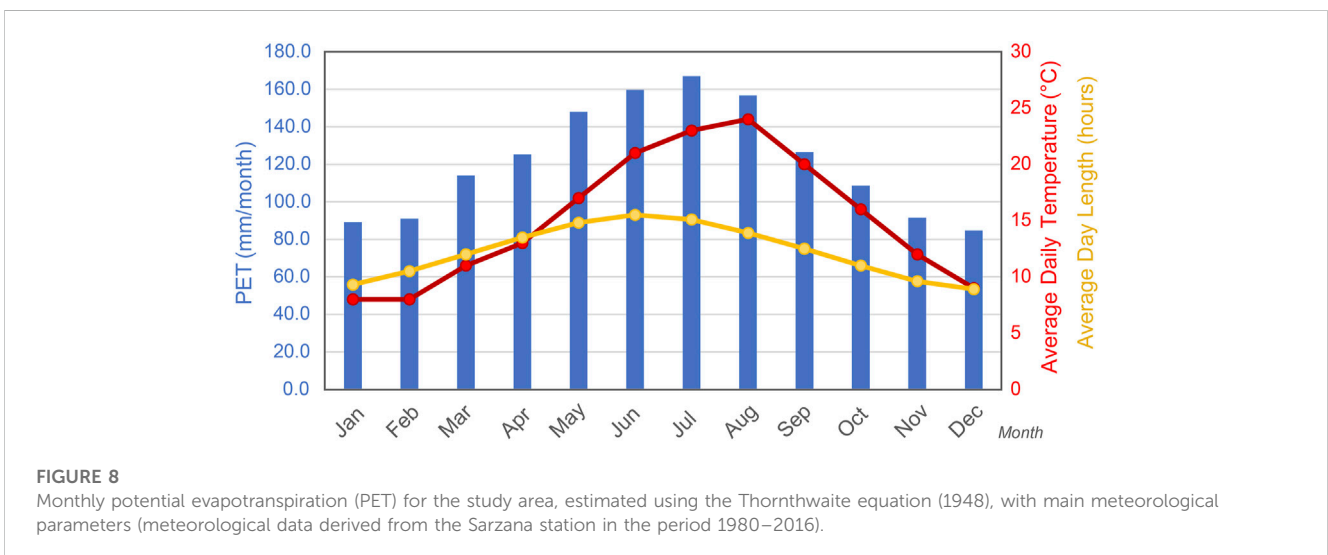
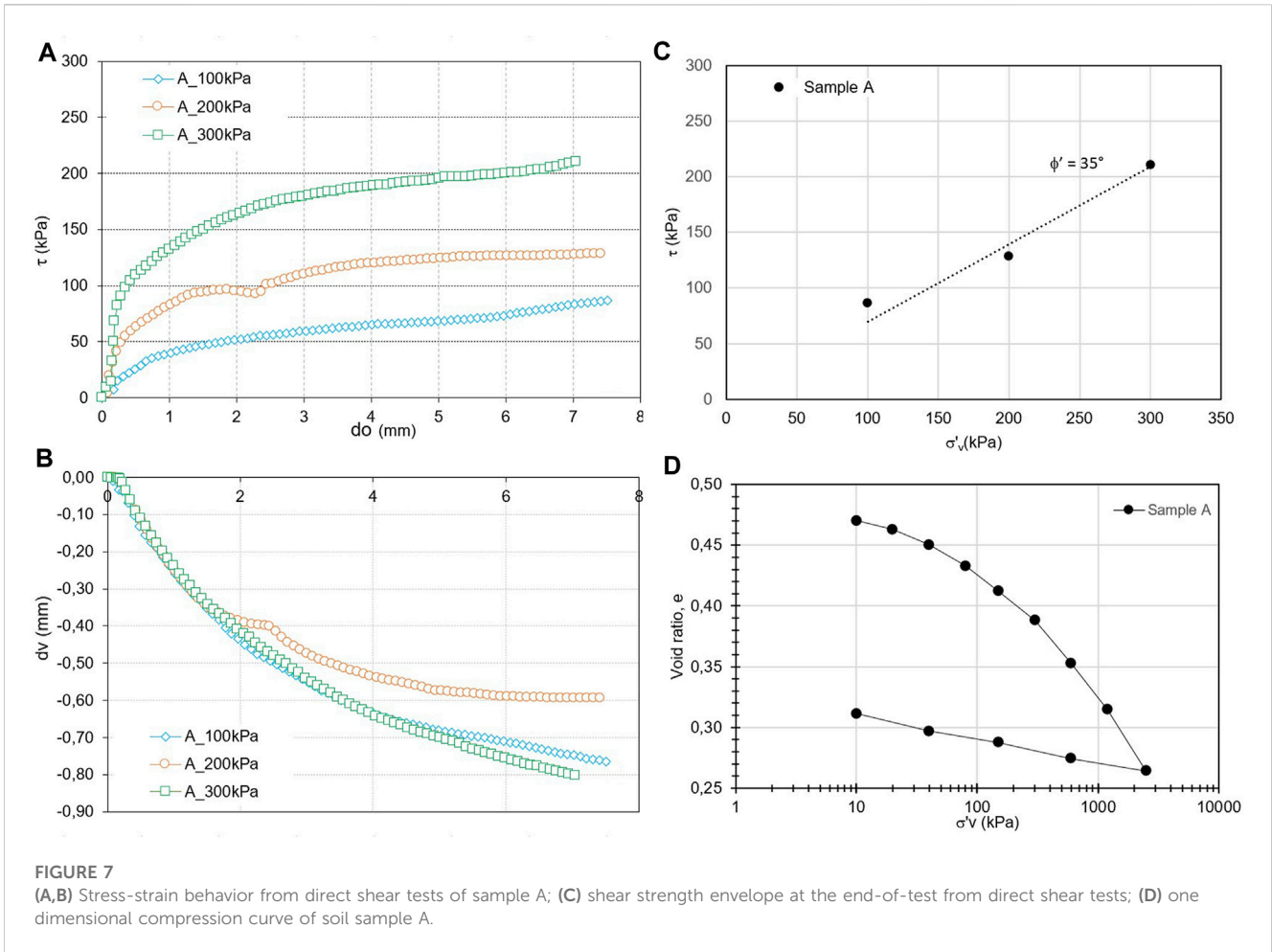


the shear strength parameters shows a friction angle of about 35° with a cohesion intercept of zero. One dimensional compressibility curve of soil is reported in Figure 7D. Compression index (Cc) and swelling index (Cs) values of respectively 0.23 and 0.034 were obtained from the compression tests on specimens having an average initial void ratio of $e_0 = 0.70$. The yield stress value determined by Casagrande method was found equal to 80 kPa.

4.3 Meteorological and soil hydrological monitoring data

The availability of more than 2 years of monitoring data allowed to analyze the variation of the soil hydraulic parameters during the different seasonal cycles, thus making possible to draw some preliminary considerations on the hydraulic response of the soil itself following changing weather conditions. The site monitoring data should be placed within a typical climatological framework for the study area, whose peculiar characteristics are summarized in Figure 8. In particular, this figure shows the potential for evapotranspiration (PET), which can directly influence the quantity of water infiltrating the soil during rainfall. The PET was calculated by applying Thornthwaite’s equation (Thornthwaite, 1948) and considering meteorological data from site monitoring or catalogues freely available online at <https://weatherspark.com/>.

In addition to a typical daily and seasonal periodic and cyclical trend, the observed temperature data showed thermal excursions in air above 30°C (Figure 9A). The daily temperature range is less evident inside the soil, reaching approximately 30°C in summer and always remaining above 10°C even in colder periods (Figure 9A). Regarding the pluviometric regime of the



study area, it is possible to notice that in summer and autumn periods, rainfall events were often characterized by short duration but high intensity, as highlighted by the hourly rainfall peaks reached, as example, on 14 August 2018 (60 mm/h), 27 October 2018 (47 mm/h), 29 October 2018

(67 mm/h) and on 27 July 2019 (40 mm/h). In particular, the event between 27–29 October 2018, led to about 220 mm of rainfall accumulation in just 3 days, thus representing the strongest event during the monitored period (Figure 9B). Also, during the second monitoring period, two severe pluviometric

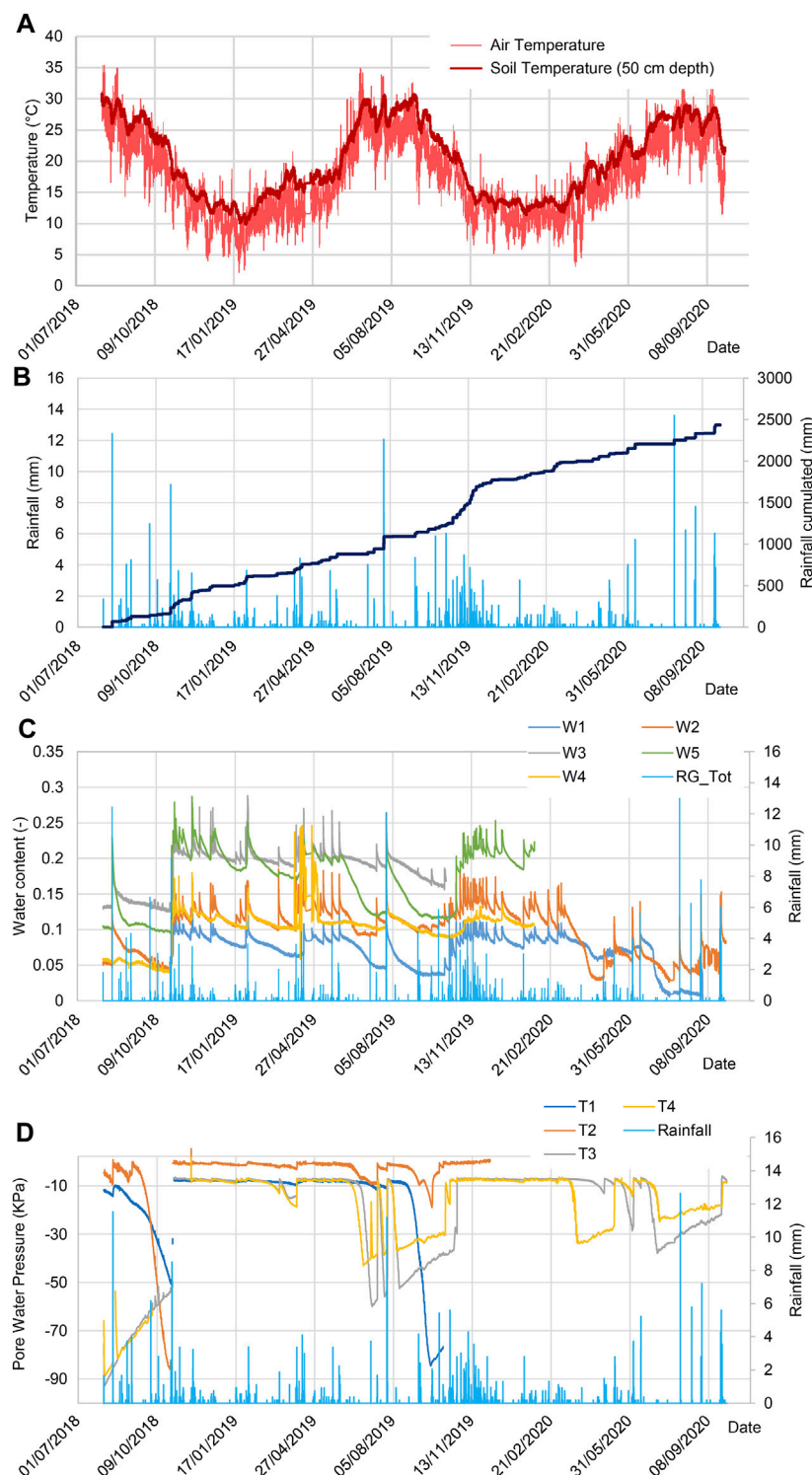


FIGURE 9 Multi-parametric data acquired during the first sensors configuration (2018–2020): **(A)** air and soil temperature, **(B)** rainfall, **(C)** water content (W) and **(D)** pore water pressure data (T). All data were graphed with a resolution of 5 min, equal to the sampling rate of the monitoring station.

events occurred on 3 November 2022, and 16 January 2023, that reached 30 mm/h (Figure 10B).

During the observation periods, both soil moisture sensors and tensiometers responded almost instantly to rainfall peaks. However, the achieved values varied according to depth. For example, sensors

W1 and T1 (placed at a depth of 100 cm b.g.l.) are those which, on average, recorded the lowest humidity and pore water pressure values, identifying a relatively drier portion of soil. Regarding pore water pressure, it can also be noted that negative values were found until the first autumn rainfall event, following which all the sensors recorded

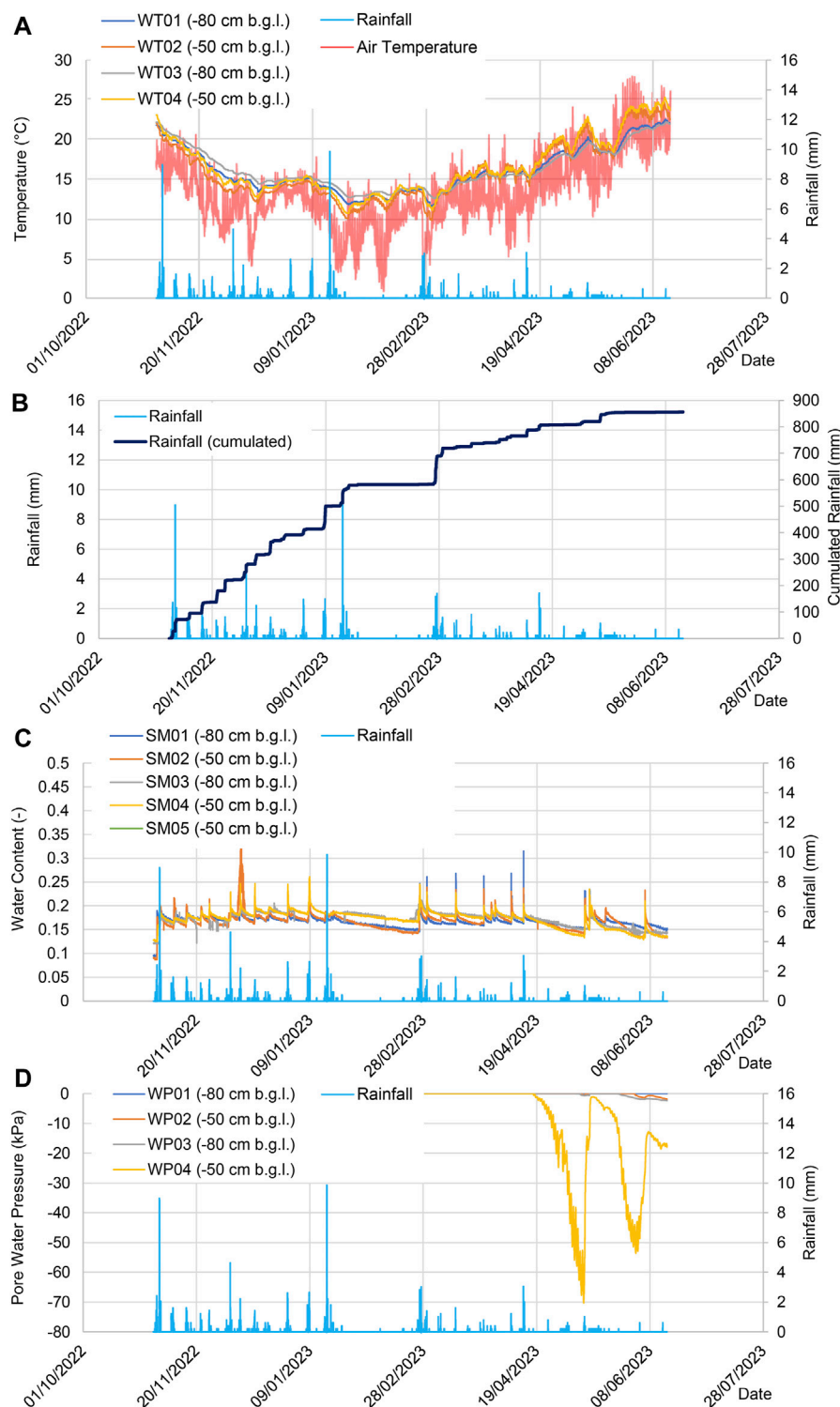


FIGURE 10

Multi-parametric data acquired during the second sensors configuration (2022 - to date): (A) air and soil temperature (WT), (B) rainfall, (C) water content (SM) and (D) pore water pressure data (WP). All data were graphed with a resolution of 5 min, equal to the sampling rate of the monitoring station.

a value close to zero throughout the winter period (Figure 9). Moreover, thanks to the temperature probes installed in the second monitoring period, at deeper soil levels, it is possible to see how during dry periods the soil temperatures remain constant down to a depth of 80 cm, while,

in wet periods, soil temperatures drop at the surface (-50 cm b.g.l.) and remain constantly higher at depth (-80 cm b.g.l.) (Figure 10). This suggests how rainfall directly induces sudden drops in the air and then in the soil temperature.

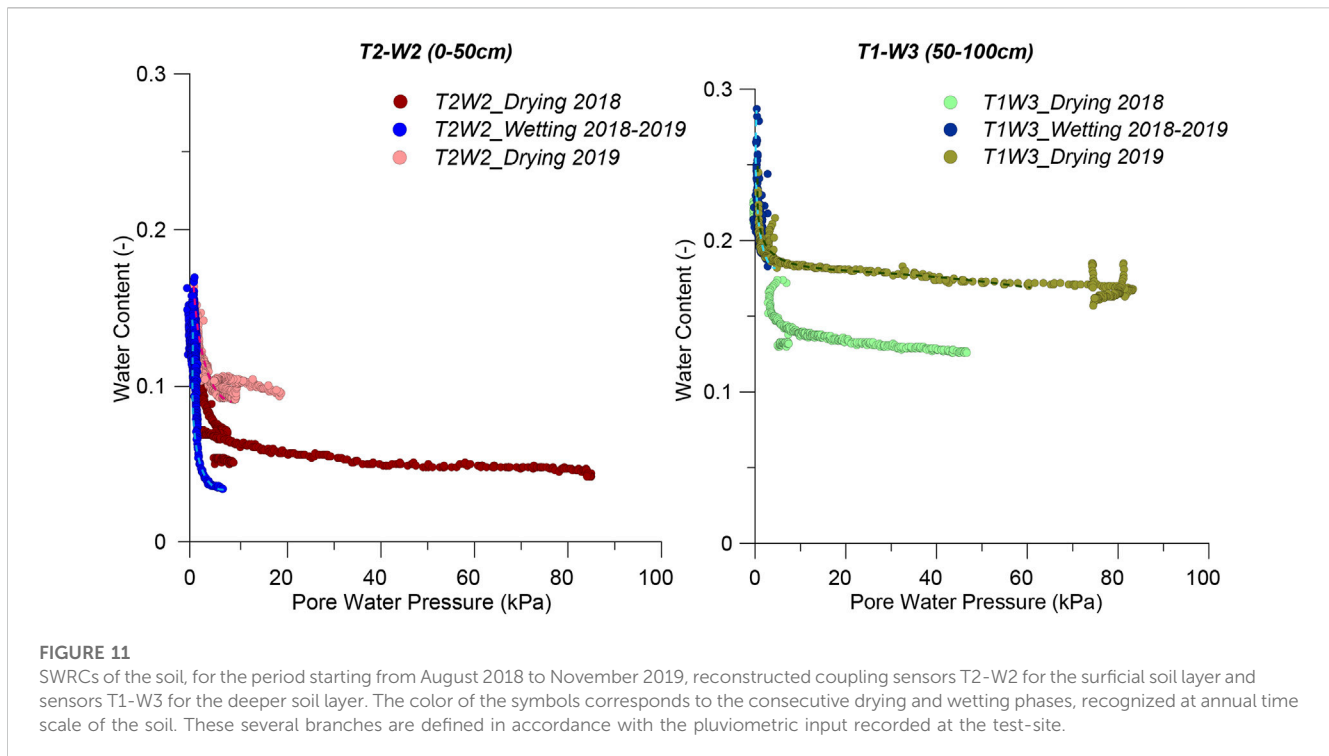


FIGURE 11

SWRCs of the soil, for the period starting from August 2018 to November 2019, reconstructed coupling sensors T2-W2 for the surficial soil layer and sensors T1-W3 for the deeper soil layer. The color of the symbols corresponds to the consecutive drying and wetting phases, recognized at annual time scale of the soil. These several branches are defined in accordance with the pluviometric input recorded at the test-site.

Finally, as a general consideration, in both monitoring periods, marked differences between the trends of soil temperature and saturation during wet phases, and those of pore water pressure in dry periods, were observed. The results are robust for the monitoring period held up to 2020. Regarding the second monitoring data series, particularly those associated with the hydraulic soil conditions, which have been recorded since October 2022, the reliability is even lower as the new sensors have had a long period of stabilization and, probably, not yet completely exhausted. This is particularly evident for soil water potential sensors that, with the exception of WP4 sensor, recorded pore water pressure values around zero even at the beginning of the drying phase in the spring of 2023 (Figure 10). If, on the one hand, this could be plausible, as WP4 was installed in the most surficial soil layer and in the downstream portion of the terrace, on the other one, it cannot be excluded that this type of sensor is equally sensitive, compared to the tensiometers, in recording the variation of pore water pressure in these soil types. It is, therefore, necessary to have the record of an entire year, i.e., the wetting and drying phases of the soil, to be able to make reliable statements about it.

Taking into consideration the time series belonging to the first monitoring period (from August 2018- to November 2019), it was possible to investigate the soil hydraulic behavior through the reconstruction of the SWRCs, which were obtained by crossing point-by-point the pore water pressure and water content values measured at the two investigated depths (i.e., 0–50 cm depth by coupling T2-W2 sensors and 50–100 cm depth by coupling T1-W3 sensors; Figure 11). The trend of the curves offers an overview of the hydrological properties of the soil. This specific case highlights a different response of the soil between the dry and wet seasons, testifying a seasonal variation of the soil parameters. Based on the rainfall data series, two drying and one wetting phases were

recognized for the analysis presented herein (following the approach proposed by Comegna et al., 2021), respectively. Specifically, starting from the first day of monitoring, which occurred on 2 August 2018, an initial drying phase lasted until 2 November 2018, the day of the first significant storm event that resulted in saturated soil conditions. Then, a wetting phase lasted until 14 June 2019, when the recovery of unsaturated conditions downstream of the winter period was observed. This condition was evident until 3 November 2019, when a significant amount of rainfall again saturated the soil. Therefore, it was possible to distinguish soil drying phases, which occur more slowly and involve the progressive decrease of the pore water pressure and the decrease of water content values, from wetting phases, which arise almost instantaneously following the first intense autumn rainfall and remain so throughout the autumn-winter season, showing pore water pressure values close to zero and higher soil saturation values. The rapidity in soil saturation, testified by the jump in the SWRCs between unsaturated and saturated conditions that occur during the primary rainfall input, can be related to the high hydraulic conductivity values typical of coarse-grained soils. Previous studies have attested this value in the order of 10^{-5} – 10^{-6} m/s (Schilirò et al., 2023). In wetting periods, the water content produced by rainfall infiltration corresponded to a specific water pressure value, which was lower than that resulting from the same soil moisture level in drying periods. The two kinds of phases are clearly visible at both depths, even if with different water content conditions, whose magnitude is strictly dependent on total cumulative rainfall along with the advance of a wetting front (Figure 11).

Based on the SWRCs reconstructed using the monitored data collected at the two selected depths, a logarithmic fitting was performed to obtain the unsaturated hydraulic properties of the soil (Table 1) according to hydraulic models proposed by

TABLE 1 Parameters of **van Genuchten (1980)** and **Kosugi (1999)** models resulting from the fitting procedure of T2–W2 and T1–W3 data on SWRCs by field monitoring, considering both 2019 drying and 2018–2019 wetting phases of the soil.

Sensor pairs: T2–W2 (depth interval: 0–50 cm)			Sensor pairs: T1–W3 (depth interval: 50–100 cm)		
Model	Parameters	R^2	Model	Parameters	R^2
van Genuchten (1980)	$\theta_{sw} (-) = 0.16125$	$R^2_w = 0.9975$	van Genuchten (1980)	$\theta_{sw} (-) = 0.29588$	$R^2_w = 0.9990$
	$\theta_{sd} (-) = 0.16576$			$\theta_{sd} (-) = 0.37774$	
	$\theta_{rw} (-) = 0.044959$			$\theta_{rw} (-) = 0.18144$	
	$\theta_{rd} (-) = 0.097953$			$\theta_{rd} (-) = 0.16993$	
	$\alpha_w (cm^{-1}) = 0.63267$	$R^2_d = 0.9778$		$\alpha_w (cm^{-1}) = 0.27232$	$R^2_d = 0.9575$
	$\alpha_d (cm^{-1}) = 0.34137$			$\alpha_d (cm^{-1}) = 1.0023$	
	$n_w (-) = 1.246$			$n_w (-) = 2.4498$	
	$n_d (-) = 1.7975$			$n_d (-) = 1.6237$	
Kosugi (1999)	$\theta_{sw} (-) = 0.16185$	$R^2_w = 0.9980$	Kosugi (1999)	$\theta_{sw} (-) = 0.31112$	$R^2_w = 0.9882$
	$\theta_{sd} (-) = 0.17557$			$\theta_{sd} (-) = 0.37774$	
	$\theta_{rw} (-) = 0.084862$			$\theta_{rw} (-) = 0.18562$	
	$\theta_{rd} (-) = 0.10027$			$\theta_{rd} (-) = 0.17233$	
	$h_{mw} (cm) = 7.0413$	$R^2_d = 0.9732$		$h_{mw} (cm) = 4.2768$	$R^2_d = 0.9446$
	$h_{md} (cm) = 4.543$			$h_{md} (cm) = 1.7197$	
	$\sigma_w (-) = 1.8143$			$\sigma_w (-) = 0.89307$	
	$\sigma_d (-) = 1.5219$			$\sigma_d (-) = 2.398$	

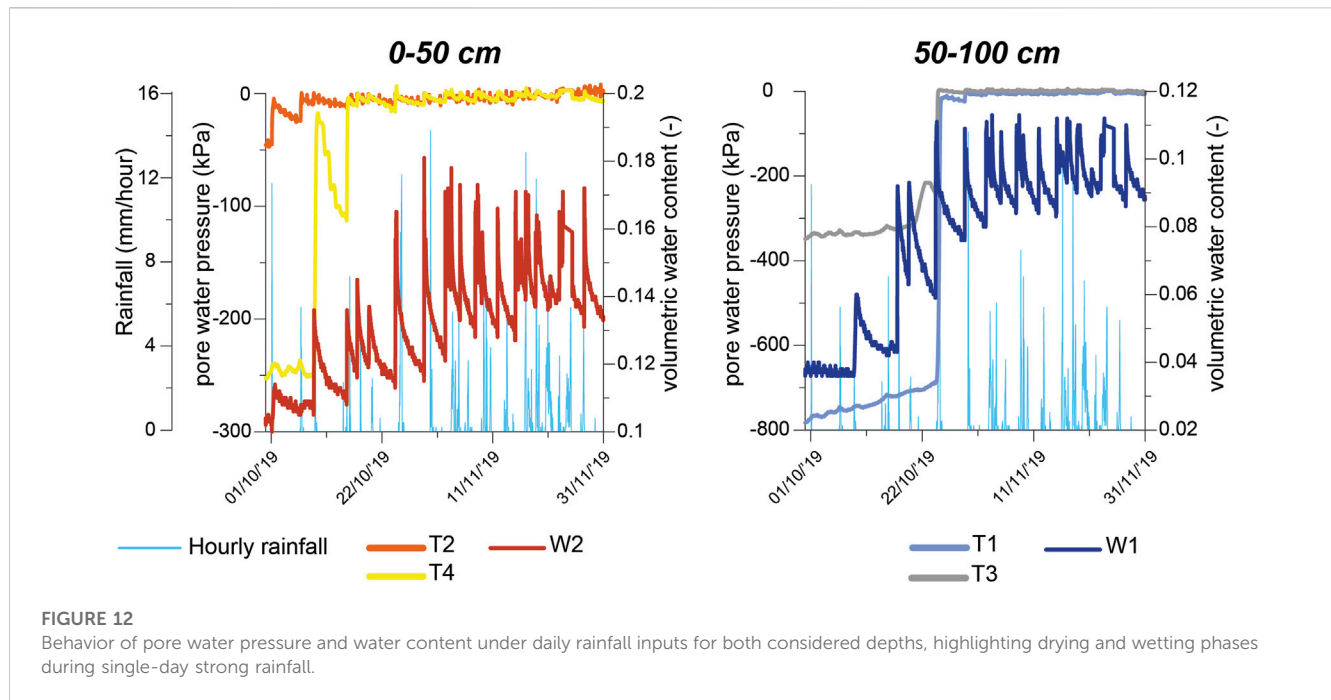
van Genuchten (1980) and Kosugi (1999). To do this, all the pairs of parameters belonging to the 2019 drying phase and 2018–2019 wetting phase of the soil were considered. Given the experimental setup, such parameters can be retained as representative of the hydraulic process acting on terraced slopes sustained by dry walls. The high R^2 values testify the reliability of the adopted fitting procedure (Table 1).

5 Discussion

Although hydrological functions of agricultural terraced systems are widely investigated in literature, there has been little examination of the role of geotechnical features of the backfill material in influencing the dynamic of infiltration (Camera et al., 2012; Arnáez et al., 2015; Preti et al., 2018a; b). From the geotechnical point of view, these soils can be considered halfway between natural and artificial materials, especially concerning their stratigraphical and textural features, which are the result of man-made reworking connected to terrace benches construction and, subsequently, to farmland activities. Indeed, terraced soils are commonly defined as constructed pedo-environments (Stanchi et al., 2012). Moreover, it is worth noting that examples concerning the hydraulic behavior of terrace backfill made up of coarse-grained soils are very rare (Camera et al., 2012). This primarily depends on the difficulties in collecting undisturbed soil samples for laboratory testing (Vannucci et al., 2019). Furthermore, in terraced landscapes, the execution of *in-situ* tests can be sometimes constrained by the rugged morphological conditions (D’Amato Avanzi et al., 2013; Cevasco et al., 2013; Cevasco et al., 2014).

In this work, investigations of the rainwater infiltration mechanisms of the monitored terraced soils were supported by the integration of *in-situ* and laboratory tests. Their outcomes revealed that soils have a well-graded texture since they consist of heterogeneous mixtures of sandy and silty-clayey gravels. However, the proportion of coarse elements is predominant, namely, the amount of gravel can be as high as 60%, while the quantity of fine soils (i.e., silt and clay) is lower than 30%. These results are well consistent with those obtained in other studies dealing with the geotechnical characterization of terraced soils at Cinque Terre (Cevasco et al., 2013b; Cevasco et al., 2014) and at zones of the Liguria region with similar geological and geomorphological settings (Cevasco et al., 2015b; 2017; Vannucci et al., 2019). The tested backfill soils resulted porous, loose and characterized by low plasticity, clearly indicating their permeable character. In this regard, Cevasco et al. (2014), using *in-situ* permeability tests, determined values of saturated hydraulic conductivity ranging from 10^{-4} to 10^{-6} m/s across soil profiles approximately 1 m-thick. Indeed, these values are in good agreement with those obtained through numerical simulations in another study performed in the same monitoring site (Schilirò et al., 2023).

The developed geotechnical framework undoubtedly affects the soil’s hydrogeological behavior, suggesting that saturation may be rapid in case of rainfall. Hydrological monitoring data retrieved from continuous time series confirmed this in the field, showing fast changes in pore water pressure and a peculiar behavior that results from both the presence of terraces and the coarse grain size distribution. At this aim, the study of SRWCs from field data



suggested that soil saturation is almost contextual to rainfall episodes, both on the small (seasonal) and on the large (daily) time window. In agricultural terraces, a similar behavior was reported by Preti et al. (2018a), who pointed out the influence of subsoil features in rainwater movement, highlighting the role of granulometric heterogeneity and of high stoniness in favoring rapid infiltration along with marked subsurface flows. The fitting of the points describing the SWRCs, on which the van Genuchten model (1980) was applied, returned hydraulic parameters in agreement with other studies in the literature, which considered soils with physical properties like those of the case study presented here (Cuomo and Della Sala, 2013; Likos et al., 2014).

With reference to the seasonal trend of rainfall, thus adopting a large time scale of analysis, it is possible to recognize an extended drying phase in the soil, which essentially involves spring, summer and the beginning of autumn, and a wetting phase that begins with the first copious autumn rainfall and continues throughout the winter, resulting in a period in which pore water pressure is constantly kept at zero at both depths considered. This seasonality suggests an influence on the extent of the apparent cohesion and, consequently, on the stability conditions of the slope. In fact, during periods when the soil is constantly wet, the contribution of negative pore water pressure to soil effective stress is expected to disappear, causing a loss in unsaturated shear strength, and thus negatively influencing slope stability (Raimondi et al., 2023; Schilirò et al., 2023). Considering the daily strong rainfall, thus adopting a small time scale of analysis, it appears to be like the same. When rainfall occurs, the pore water pressure increases and almost instantly reaches higher values, especially in the uppermost soil layer. The same instantaneous impulse is also shown by water content, which tends to increase faster. At greater depths, the increase in pore water pressure is recorded with a few days of delay or, if it continuously rains over time, while the water content shown the same behavior as at upper

depth (Figure 12). Anyway, the lag time between the pluviometric input and the soil response in terms of change of the hydraulic parameters is very short. Furthermore, regarding both the pore water pressure and water content, a certain degree of data scattering can be noticed considering daily time windows. The cause can be ascribed to hysteresis processes occurring after more intense rainfall (Likos et al., 2014; Bordoni et al., 2015; Comegna et al., 2021; Darzi et al., 2023).

As regards the hydraulic conditions of the soil along the investigated section (i.e., considering both the geometry of the slope and of the terrace bench itself with an average inclination of 27°), it is possible to notice that, in the downslope portion (Figures 3, 9), higher water content values are recorded than those acquired in the upslope portion (i.e., at the same depth b.g.l.). At the investigated terraced site, this hydrological evidence coming from field monitoring may be explained through a wetting front infiltration scheme, recently proposed by Schilirò et al. (2023), according to which the infiltrating water tends to accumulate on the lower edge of the terrace. Following this scheme, an increase in pore water pressure occurs in the shallower soil layer during rainfall, and, if rain continues, positive pore water pressure can also develop.

6 Conclusion

The knowledge of the hydrological features of the backfill soil of agricultural terraces is of fundamental importance for several practical and scientific reasons. On the one hand, understanding water circulation through terraced soils can have important implications in improving strategies of water cycle regulation, thus contributing to the effective maintenance and management of terraced landscapes. On the other hand, investigation of the links between meteorological stressors and hydrological mechanisms, as

well as cause-to-effect relationship with erosion and mass movements processes, can support the calibration of hydro-meteorological trigger thresholds for the shallow landslides in the frame of early-warning systems. However, because of local geo-environmental and anthropic factors, the hydro-geomorphological functions of terraces can be extremely peculiar and variable, thus requiring both site specific analysis and the availability of long-term monitoring, to be transferred in distributed analysis of scenarios.

In light of these considerations, in the site of Monterosso al Mare the coupling of engineering-geological information with multi-sensor hydrological monitoring data, which covered an observation period longer than 2 years, allowed to define the stratigraphic and geotechnical model of an agricultural terrace and its influence on the hydro-mechanical behavior of the backfill soils.

The main results of the study showed that the coarse-grained and anthropically remolded texture of the backfill soil promotes the rapid infiltration of rainwater, causing sharp changes in both water content and pore water pressure, especially in the shallower and looser horizons. Furthermore, both the nature and the texture of the backfill soil also influence the pattern of water content and pore water pressure, which revealed a peculiar seasonal trend characterized by alternating phases of slow drying and fast wetting. Accordingly, during the drying periods, typically developing in the spring and summer seasons, a progressive decrease in pore water pressure occurs, suggesting a positive contribute to the shear strength of soils in terms of apparent cohesion. Conversely, during the wetting phases, arising almost instantaneously at the time of the first intense autumn rainstorms, soils reach greater saturation conditions while pore water pressure remains close to zero throughout the autumn-winter season, thus producing hydro-mechanical conditions that could negatively influence the stability of the backfill soil. The outlined hydrological patterns are observable both in shallower and deeper soil horizons. However, monitoring data reveal that the greater water accumulations can develop towards the lower portion of the terrace tread. This may induce the growth of destabilizing pore water pressure regimes into the soil volume behind the dry-stone wall.

Data availability statement

The original contributions presented in the study are included in the article/Supplementary material, further inquiries can be directed to the corresponding author.

Author contributions

MF: Conceptualization, Data curation, Formal Analysis, Investigation, Methodology, Writing—original draft. GP: Conceptualization, Data curation, Formal Analysis, Investigation, Methodology, Writing—original draft. GM: Conceptualization, Data curation, Formal Analysis, Investigation, Methodology, Writing—original draft. MP: Funding acquisition, Writing—review and editing. DD: Conceptualization, Writing—review and editing. LG: Investigation, Writing—review and editing. GB: Investigation,

Writing—review and editing. EV: Conceptualization, Data curation, Formal Analysis, Investigation, Methodology, Writing—original draft. ER: Data curation, Investigation, Writing—review and editing. LR: Data curation, Investigation, Writing—review and editing. AC: Conceptualization, Investigation, Methodology, Supervision, Writing—review and editing. DC: Supervision, Writing—review and editing. GS: Funding acquisition, Project administration, Supervision, Writing—review and editing.

Funding

The author(s) declare financial support was received for the research, authorship, and/or publication of this article. This research was funded by the project “Grandi frane in roccia e frane superficiali a cinematica rapida in aree montane: metodi per la previsione temporale e spaziale (prediction and susceptibility)” by DARA—Dipartimento per gli Affari Regionali e le Autonomie within the Convention in co-operation between DARA and Earth Sciences Department, Sapienza University, and it was partly carried out within the RETURN Extended Partnership and received funding from the European Union Next-GenerationEU (National Recovery and Resilience Plan—NRRP, Mission 4, Component 2, Investment 1.3—DD 1243 2/8/2022, PE0000005). Paper printed with the financial support of the PRIN (Progetti di Rilevante Interesse Nazionale—Projects of National Relevant Interest) URGENT (Urban Geology and Geohazards: Engineering geology for safer, resilient and smart ciTies) project (Principal Investigator of the research unit: DC).

Acknowledgments

The authors would like to thank Cinque Terre National Park for providing logistic support during the installation of the monitoring equipment. The authors are also grateful to the reviewers for their constructive comments and suggestions that improved the quality of this paper.

Conflict of interest

The authors declare that the research was conducted in the absence of any commercial or financial relationships that could be construed as a potential conflict of interest.

The author(s) declared that they were an editorial board member of *Frontiers*, at the time of submission. This had no impact on the peer review process and the final decision.

Publisher's note

All claims expressed in this article are solely those of the authors and do not necessarily represent those of their affiliated organizations, or those of the publisher, the editors and the reviewers. Any product that may be evaluated in this article, or claim that may be made by its manufacturer, is not guaranteed or endorsed by the publisher.

References

- Abbate, E., Fanucci, F., Benvenuti, M., Bruni, P., Cipriani, N., Falorni, P., et al. (2005). *Carta Geologica d'Italia alla scala 1:50.000-Foglio 248- La Spezia con note illustrative*. Genova: Regione Liguria - Dipartimento Ambiente Edilizia e Lavori Pubblici, Servizio Politiche dell'Assetto Territoriale, 1–204.
- Agnoletti, M., Errico, A., Santoro, A., Dani, A., and Preti, F. (2019). Terraced landscapes and hydrogeological risk. Effects of land abandonment in Cinque Terre (Italy) during severe rainfall events. *Sustainability* 11, 235. doi:10.3390/su11010235
- Arnáez, J., Lana Renault, N., Lasanta, T., Ruiz Flaño, P., and Castroviejo, J. (2015). Effects of farming terraces on hydrological and geomorphological processes. A review. *Catena* 128, 122–134. doi:10.1016/j.catena.2015.01.021
- ASTM Committee on Standards, (1988). *ASTM standard test methods d854-02 for specific gravity of soils*. West Conshohocken, PA, USA: ASTM International.
- ASTM Committee on Standards, (2000). *ASTM standard test method D 4959-00 for determination of water (moisture) content of soil by direct heating*. West Conshohocken, PA, USA: ASTM International.
- ASTM Committee on Standards, (2000). *ASTM standard test method d422-63 for particle-size analysis of soils*. West Conshohocken, PA, USA: ASTM International.
- ASTM Committee on Standards (2007). *ASTM standard test method d1556-07 for density and unit weight of soil in place by the sand-cone method*. West Conshohocken, PA, USA: ASTM International.
- ASTM Committee on Standards (2010). *ASTM standard test methods d4318-10 for liquid limit, plastic limit, and plasticity index of soils*. West Conshohocken, PA, USA: ASTM International.
- ASTM Committee on Standards (2014). *ASTM standard test methods d2974-14 for moisture, ash, and organic matter of peat and other organic soils*. West Conshohocken, PA, USA: ASTM International.
- Bogaard, T. A., and Greco, R. (2016). Landslide hydrology: from hydrology to pore pressure. *Wires Water* 3, 439–459. doi:10.1002/wat2.1126
- Bordoni, M., Meisina, C., Valentino, R., Lu, N., Bittelli, M., and Chersich, S. (2015). Hydrological factors affecting rainfall-induced shallow landslides: from the field monitoring to a simplified slope stability analysis. *Eng. Geol.* 193, 19–37. doi:10.1016/j.enggeo.2015.04.006
- Brandolini, P. (2017). “The outstanding terraced landscape of the Cinque Terre coastal slopes (eastern Liguria),” in *Landforms and landscapes of Italy*. Editors M. Soldati and M. Marchetti (Cham, Switzerland: Springer International), 235–244. doi:10.1007/978-3-319-26194-2_20
- Cambi, M., Giambastiani, Y., Giannetti, F., Nuti, E., Dani, A., and Preti, F. (2021). Integrated low-cost approach for measuring the state of conservation of agricultural terraces in tuscan, Italy. *Italy. Water* 13 (2), 113. doi:10.3390/w13020113
- Camera, C., Apuani, T., and Masetti, M. (2014). Mechanisms of failure on terraced slopes: the Valtellina case (northern Italy). *Landslides* 11, 43–54. doi:10.1007/s10346-012-0371-3
- Camera, C., Masetti, M., and Apuani, T. (2012). Rainfall, infiltration, and groundwater flow in a terraced slope of Valtellina (Northern Italy): field data and modelling. *Environ. Earth Sci.* 65 (4), 1191–1202. doi:10.1007/s12665-011-1367-3
- Cardinali, M., Galli, M., Guzzetti, F., Ardizzone, F., Reichenbach, P., and Bartocchini, P. (2006). Rainfall induced landslides in December 2004 in south-western Umbria, central Italy: types, extent, damage and risk assessment. *Nat. Hazards Earth Syst. Sci.* 6 (2), 237–260. doi:10.5194/nhess-6-237-2006
- Cascini, L., Cuomo, S., and Guida, D. (2008). Typical source areas of May 1998 flow-like mass movements in the Campania region, Southern Italy. *South. Italy. Eng. Geol.* 96, 107–125. doi:10.1016/j.enggeo.2007.10.003
- Cevasco, A., Brandolini, P., Scopesi, C., and Rellini, I. (2013a). Relationships between geo-hydrological processes induced by heavy rainfall and land-use: the case of 25 October 2011 in the Vernazza catchment (Cinque Terre, NW Italy). *J. Maps* 9 (2), 289–298. doi:10.1080/17445647.2013.780188
- Cevasco, A., Diodato, N., Revellino, P., Fiorillo, F., Grelle, G., and Guadagno, F. M. (2015a). Storminess and geo-hydrological events affecting small coastal basins in a terraced Mediterranean environment. *Sci. Total Environ.* 532, 208–219. doi:10.1016/j.scitotenv.2015.06.017
- Cevasco, A., Pepe, G., and Brandolini, P. (2013b). Geotechnical and stratigraphic aspects of shallow landslides at Cinque Terre (Liguria, Italy). *Rend. Online Soc. Geol. It.* 24, 52–54.
- Cevasco, A., Pepe, G., and Brandolini, P. (2014). The influences of geological and land use settings on shallow landslides triggered by an intense rainfall event in a coastal terraced environment. *Bull. Eng. Geol. Environ.* 73, 859–875. doi:10.1007/s10064-013-0544-x
- Cevasco, A., Pepe, G., D'Amato Avanzi, G., and Giannecchini, R. (2015b). A study on the 10 November 2014 intense rainfall and the related landslides in the lower Lavagna valley (eastern Liguria). *Rend. Online Soc. Geol. It.* 35, 66–69. doi:10.3301/ROL.2015.65
- Cevasco, A., Pepe, G., D'Amato Avanzi, G., and Giannecchini, R. (2017). Preliminary analysis of the November 10, 2014 rainstorm and related landslides in the lower Lavagna valley (Eastern Liguria). *Ital. J. Eng. Geol. Env. Spec. Issue* 1, 5–15. doi:10.4408/IJEGE.2017-01-S-01
- Coelho, N. A. L., Sato, A. M., Avelar, A. S., Vianna, L. G. G., Araujo, I. S., Croix, D., et al. (2011). “The extreme landslide disaster in Brazil,” in *Proc. 2nd World landslides forum* (Berlin, Germany: Springer).
- Collins, B. D., and Znidarcic, D. (2004). Stability analyses of rainfall induced landslides. *J. Geotech. Geoenv. Eng.* 130 (4), 362–372. doi:10.1061/(asce)1090-0241(2004)130:4(362)
- Comegna, L., Damiano, E., Greco, R., Olivares, L., and Picarelli, L. (2021). The hysteretic response of a shallow pyroclastic deposit. *Earth Syst. Sci. Data* 13 (6), 2541–2553. doi:10.5194/essd-13-2541-2021
- Crosta, G. (1998). Regionalization of rainfall thresholds: an aid to landslide hazard evaluation. *Env. Geol.* 35 (2-3), 131–145. doi:10.1007/s002540050300
- Crosta, G. B., Negro, P. D., and Frattini, P. (2003). Soil slips and debris flows on terraced slopes. *Nat. Hazards Earth Syst. Sci.* 3 (1/2), 31–42. doi:10.5194/nhess-3-31-2003
- Crozier, M. J. (2005). Multiple-occurrence regional landslide events in New Zealand: hazard management issues. *Landslides* 2 (4), 247–256. doi:10.1007/s10346-005-0019-7
- Cuomo, S., and Della Sala, M. (2013). Rainfall-induced infiltration, runoff and failure in steep unsaturated shallow soil deposits. *Eng. Geol.* 162, 118–127. doi:10.1016/j.enggeo.2013.05.010
- Dai, F. C., and Lee, C. F. (2002). Landslide characteristics and slope instability modeling using GIS, Lantau Island, Hong Kong. *Geomorphology* 42, 213–228. doi:10.1016/S0169-555X(01)00087-3
- D'Amato Avanzi, G., Galanti, Y., Giannecchini, R., Lo Presti, D., and Puccinelli, A. (2013). Estimation of soil properties of shallow landslide source areas by dynamic penetration tests: first outcomes from Northern Tuscany (Italy). *Bull. Eng. Geol. Environ.* 72, 609–624. doi:10.1007/s10064-013-0535-y
- Darzi, A. G., Sadeghi, H., and Zhou, C. (2023). A soil-brine retention model for wetting processes considering the hysteresis effects. *Transp. Geotech.* 41, 101032. doi:10.1016/j.trgeot.2023.101032
- Dietrich, W. E., Wilson, C. J., and Reneau, S. L. (1986). “Hollows, colluvium and landslides in soil mantled landscapes,” in *Hillslope processes*. Editor A. D. Abrahams (London, UK: Allen & Unwin), 361–385.
- Fannin, R. J., and Jaakkola, J. (1999). Hydrological response of hillslope soils above a debris-slide headscarp. *Can. Geotech. J.* 36 (6), 1111–1122. doi:10.1139/t99-074
- Fiorucci, M., Martino, S., Bozzano, F., and Prestininzi, A. (2020). Comparison of approaches for data analysis of multi-parametric monitoring systems: insights from the Acuto test-site (Central Italy). *Appl. Sci.* 10 (21), 7658. doi:10.3390/app10217658
- Freer, J., McDonnell, J. J., Beven, K. J., Peters, N. E., Burns, D. A., Hooper, R. P., et al. (2002). The role of bedrock topography on subsurface storm flow. *Water Resour. Res.* 38 (12), 1269. doi:10.1029/2001WR000872
- Fuchu, D., Lee, C. F., and Sijing, W. (1999). Analysis of rainstorm-induced slide-debris flows on natural terrain of Lantau Island, Hong Kong. *Eng. Geol.* 51 (4), 279–290. doi:10.1016/S0013-7952(98)00047-7
- Galanti, Y., Barsanti, M., Cevasco, A., D'Amato Avanzi, G., and Giannecchini, R. (2018). Comparison of statistical methods and multi-time validation for the determination of the shallow landslide rainfall thresholds. *Landslides* 15, 937–952. doi:10.1007/s10346-017-0919-3
- Gallart, F., Latron, J., Llorens, P., and Rabada, D. (1997). Hydrological functioning of Mediterranean mountain basins in Vallcebre, Catalonia: some challenges for hydrological modelling. *Hydrol. Process.* 11, 1263–1272. doi:10.1002/(sici)1099-1085(199707)11:9<1263::aid-hyp556>3.0.co;2-w
- Galve, J. P., Cevasco, A., Brandolini, P., Piacentini, D., Azañón, J. M., Notti, D., et al. (2016). Cost-based analysis of mitigation measures for shallow-landslide risk reduction strategies. *Eng. Geol.* 213, 142–157. doi:10.1016/j.enggeo.2016.09.002
- García Ruiz, J. M., and Lana Renault, N. (2011). Hydrological and erosive consequences of farmland abandonment in Europe, with special reference to the Mediterranean region—a review. *Agric. Ecosyst. Environ.* 140, 317–338. doi:10.1016/j.agee.2011.01.003
- Gibbs, H. J., and Holtz, W. G. (1957). “Research on determining the density of sands by spoon penetration testing,” in 4th ICOSOMEF, London, 35–39.
- Giordan, D., Cignetti, M., Baldo, M., and Godone, D. (2017). Relationship between man-made environment and slope stability: the case of 2014 rainfall events in the terraced landscape of the Liguria region (northwestern Italy). *Geomat. Nat. Hazards Risk* 8, 1833–1852. doi:10.1080/19475705.2017.1391129
- Giordan, D., Cignetti, M., Godone, D., Peruccacci, S., Raso, E., Pepe, G., et al. (2020). A new procedure for an effective management of geo-hydrological risks across the “sentiero verde-azzurro” trail, Cinque Terre national park, Liguria (North-Western Italy). *Sustainability* 12 (2), 561–578. doi:10.3390/su12020561
- Godt, J. W., Baum, R. L., Savage, W. Z., Salciarini, D., Schulz, W. H., and Harp, E. L. (2008). Transient deterministic shallow landslide modeling: requirements for susceptibility and hazard assessments in a GIS framework. *Eng. Geol.* 102 (3-4), 214–226. doi:10.1016/j.enggeo.2008.03.019
- Guadagno, F. M., Forte, R., Revellino, P., Fiorillo, F., and Focareta, M. (2005). Some aspects of the initiation of debris avalanches in the Campania Region: the role of morphological slope discontinuities and the development of failure. *Geomorphology* 66, 237–254. doi:10.1016/j.geomorph.2004.09.024

- Guthrie, R. H., and Evans, S. G. (2004). Analysis of landslide frequencies and characteristics in a natural system, coastal British Columbia. *Earth Surf. Process. Landforms* 29 (11), 1321–1339. doi:10.1002/esp.1095
- Gutiérrez, F., Gutiérrez, M., and Sancho, C. (1998). Geomorphological and sedimentological analysis of a catastrophic flash flood in the Arás drainage basin (central Pyrenees, Spain). *Geomorphology* 22, 265–283. doi:10.1016/S0169-555X(97)00087-1
- Guzzetti, F., Cardinali, M., Reichenbach, P., Cipolla, F., Sebastiani, C., Galli, M., et al. (2004). Landslides triggered by the 23 november 2000 rainfall event in the imperia Province, western Liguria, Italy. *Italy. Eng. Geol.* 73, 229–245. doi:10.1016/j.enggeo.2004.01.006
- Harp, E. L., Reid, M. E., McKenna, J. P., and Michael, J. A. (2009). Mapping of hazard from rainfall-triggered landslides in developing countries: examples from Honduras and Micronesia. *Eng. Geol.* 104 (3–4), 295–311. doi:10.1016/j.enggeo.2008.11.010
- Hungar, O., Leroueil, S., and Picarelli, L. (2014). The Varnes classification of landslide types, an update. *Landslides* 11, 167–194. doi:10.1007/s10346-013-0436-y
- Iverson, R. M., and Major, J. J. (1986). Groundwater seepage vectors and the potential for hillslope failure and debris flow mobilization. *Water Resour. Res.* 22 (11), 1543–1548. doi:10.1029/wr022i011p01543
- Johnson, K. A., and Sitar, N. (1990). Hydrologic conditions leading to debris-flow initiation. *Can. Geotech. J.* 27, 789–801. doi:10.1139/t90-092
- Köppen, W. (1884). The thermal zones of the earth according to the duration of hot, moderate and cold periods and to the impact of heat on the organic world. *Meteorol. Z.* 20, 351–360. doi:10.1127/0941-2948/2011/105
- Kosugi, K. (1999). General model for unsaturated hydraulic conductivity for soils with lognormal pore-size distribution. *Soil Sci. Soc. Am. J.* 63 (2), 270–277. doi:10.2136/sssaj1999.03615995006300020003x
- Lacerda, W. A. (2007). Landslide initiation in saprolite and colluvium in southern Brazil: field and laboratory observations. *Geomorphology* 87 (3), 104–119. doi:10.1016/j.geomorph.2006.03.037
- Larsen, M. C. (2008). Rainfall-triggered landslides, anthropogenic hazards, and mitigation strategies. *Adv. Geosci.* 14, 147–153. doi:10.5194/adgeo-14-147-2008
- Larsen, M. C., and Wieczorek, G. F. (2006). Geomorphic effects of large debris flows and flash floods, northern Venezuela, 1999. *Z. Geomorph. N.F.* 145, 147–175.
- Lesschen, J. P., Cammeraat, L. H., and Nieman, T. (2008). Erosion and terrace failure due to agricultural land abandonment in a semi-arid environment. *Earth Surf. Proc. Land.* 33, 1574–1584. doi:10.1002/esp.1676
- Likos, W. J., Lu, N., and Godt, J. W. (2014). Hysteresis and uncertainty in soil water-retention curve parameters. *J. Geotech. Geoenvironmental Eng.* 140 (4), 04013050. doi:10.1061/(ASCE)GT.1943-5606.0001071
- Lu, N., and Godt, J. W. (2013). *Hillslope hydrology and stability*. Cambridge, UK: Cambridge University Press.
- Mandarino, A., Luino, F., and Faccini, F. (2021). Flood-induced ground effects and flood-water dynamics for hydro-geomorphic hazard assessment: the 21–22 October 2019 extreme flood along the lower Orba River (Alessandria, NW Italy). *J. Maps* 17 (3), 136–151. doi:10.1080/17445647.2020.1866702
- Moreno-de-las-Heras, M., Lindenberger, F., Latron, J., Lana-Renault, N., Llorens, P., Arnáez, J., et al. (2019). Hydro-geomorphological consequences of the abandonment of agricultural terraces in the Mediterranean region: key controlling factors and landscape stability patterns. *Geomorphology* 333, 73–91. doi:10.1016/j.geomorph.2019.02.014
- Nunes, J. P., Bernard Jannin, L., Rodriguez Blanco, M. L., Santos, J. M., Coelho, C. D. O. A., and Keizer, J. J. (2018). Hydrological and erosion processes in terraced fields: observations from a humid Mediterranean region in Northern Portugal. *Land Degrad. Dev.* 29 (3), 596–606. doi:10.1002/ldr.2550
- Odebrecht, E., Schnaid, F., Rocha, M. M., and Bernardes, G. P. (2005). Energy efficiency for standard penetration tests. *J. Geotech. Geoenviron. Eng.* 131 (10), 1252–1263. doi:10.1061/(asce)1090-0241(2005)131:10(1252)
- Pepe, G., Baudinelli, E., Zanini, M., Calcaterra, D., Cevasco, A., Firpo, M., et al. (2020). Application of bioengineering techniques as geo-hydrological risk mitigation measures in a highly valuable cultural landscape: experiences from the Cinque Terre national park (Italy). *Sustainability* 12, 8653. doi:10.3390/su12208653
- Pepe, G., Mandarino, A., Raso, E., Scarpellini, P., Brandolini, P., and Cevasco, A. (2019). Investigation on farmland abandonment of terraced slopes using multitemporal data sources comparison and its implication on hydro-geomorphological processes. *Water* 11 (8), 1552. doi:10.3390/w11081552
- Pijl, A., Quarella, E., Vogel, T. A., D'Agostino, V., and Tarolli, P. (2021). Remote sensing vs. field-based monitoring of agricultural terrace degradation. *Int. Soil Water Conserv. Res.* 9 (1), 1–10. doi:10.1016/j.iswcr.2020.09.001
- Preti, F., Errico, A., Caruso, M., Dani, A., and Guastini, E. (2018b). Dry-stone wall terrace monitoring and modelling. *Land Degrad. Dev.* 29 (6), 1806–1818. doi:10.1002/ldr.2926
- Preti, F., Guastini, E., Penna, D., Dani, A., Cassiani, G., Boaga, J., et al. (2018a). Conceptualization of water flow pathways in agricultural terraced landscapes. *Land Degrad. Dev.* 29 (3), 651–662. doi:10.1002/ldr.2764
- Rahardjo, H., Lim, T. T., Chang, M. F., and Fredlund, D. G. (1995). Shear strength characteristics of a residual soil. *Can. Geotech. J.* 32, 60–77. doi:10.1139/t95-005
- Raimondi, L., Pepe, G., Firpo, M., Calcaterra, D., and Cevasco, A. (2023). An open-source and QGIS-integrated physically based model for spatial prediction of rainfall-induced shallow landslides (SPRIn-SL). *Environ. Model. Softw.* 160, 105587. doi:10.1016/j.envsoft.2022.105587
- Raso, E., Cevasco, A., Di Martire, D., Pepe, G., Scarpellini, P., Calcaterra, D., et al. (2019). Landslide-inventory of the Cinque Terre national park (Italy) and quantitative interaction with the trail network. *J. Maps* 15 (2), 818–830. doi:10.1080/17445647.2019.1657511
- Raso, E., Mandarino, A., Pepe, G., Calcaterra, D., Cevasco, A., Confuorto, P., et al. (2021). Geomorphology of Cinque Terre national park (Italy). *J. Maps* 17 (3), 171–184. doi:10.1080/17445647.2020.1837270
- Regione Liguria (2022). Consultazione dati meteo-climatici. <http://www.cartografiar.regione.liguria.it/SiraQualMeteo/script/PubAccessoDatiMeteo.asp> (accessed on December 09, 2022).
- Schilirò, L., Cevasco, A., Esposito, C., and Scarascia Mugnozza, G. (2018). Shallow landslide initiation on terraced slopes: inferences from a physically-based approach. *Geomat. Nat. Haz. Risk* 9 (1), 295–324. doi:10.1080/19475705.2018.1430066
- Schilirò, L., Esposito, C., and Scarascia Mugnozza, G. (2015). Evaluation of shallow landslide-triggering scenarios through a physically based approach: an example of application in the southern Messina area (northeastern Sicily, Italy). *Nat. Hazards Earth. Syst. Sci.* 15, 2091–2109. doi:10.5194/nhess-15-2091-2015
- Schilirò, L., Marmoni, G. M., Fiorucci, M., Pecci, M., and Scarascia Mugnozza, G. (2023). Preliminary insights from hydrological field monitoring for the evaluation of landslide triggering conditions over large areas. *Nat. Hazards* 118, 1401–1426. doi:10.1007/s11069-023-06064-0
- Schilirò, L., Poueme Djueyep, G., Esposito, C., and Scarascia Mugnozza, G. (2019). The role of initial soil conditions in shallow landslide triggering: insights from physically based approaches. *Geofluids* 2019, 1–14. doi:10.1155/2019/2453786
- Scopesi, C., Olivari, S., Firpo, M., Scarpellini, P., Pini, S., and Rellini, I. (2020). Land capability classification of Vernazza catchment, Cinque Terre national park, Italy. *J. Maps* 16 (2), 357–362. doi:10.1080/17445647.2020.1750067
- Seki, K., Toride, N., and van Genuchten, M. T. (2022). Evaluation of a general model for multimodal unsaturated soil hydraulic properties. <https://arxiv.org/abs/2212.02965>.
- Sepe, C., Calcaterra, D., Di Martire, D., Fusco, F., Tufano, R., Vitale, E., et al. (2023). Triggering conditions and propagation of the December 2019 Palma Campania landslide: implications for residual hazard estimation at recurrent landslide sites. *Eng. Geol.* 322, 107177. doi:10.1016/j.enggeo.2023.107177
- Springman, S. M., Thielen, A., Kienzler, P., and Friedel, S. (2013). A long-term field study for the investigation of rainfall-induced landslides. *Geotechnique* 14, 1177–1193. doi:10.1680/geot.11.P.142
- Stanchi, S., Freppaz, M., Agnelli, A., Reinsch, T., and Zanini, E. (2012). Properties, best management practices and conservation of terraced soils in Southern Europe (from Mediterranean areas to the Alps): a review. *Quat. Int.* 265, 90–100. doi:10.1016/j.quaint.2011.09.015
- Stefanoff, G., Sanglerat, G., Bergdahl, U., and Melzer, K. J. (1988). Dynamic probing (DP): international reference test procedure. *Proceeding 1st Int. symposium penetration Test.* 1, 53–70.
- Tarolli, P., Preti, F., and Romano, N. (2014). Terraced landscapes: from an old best practice to a potential hazard for soil degradation due to land abandonment. *Anthropocene* 6, 10–25. doi:10.1016/j.ancene.2014.03.002
- Terranova, R., Brandolini, P., Spotorno, M., Rota, M., Montanari, C., Galassi, D., et al. (2002). *Patrimoni de marjades a la Mediterrània Occidental. Una proposta de catalogació. Comissió Europea DGX, Programa Raphael.* Spain: Palma Di Mallorca, 1–243.
- Thorntwaite, C. W. (1948). An approach toward a rational classification of climate. *Geogr. Rev.* 38 (1), 55–94. doi:10.2307/210739
- van Genuchten, M. T. (1980). A closed-form equation for predicting the hydraulic conductivity of unsaturated soils. *Soil Sci. Soc. Am. J.* 44 (5), 892–898. doi:10.2136/sssaj1980.03615995004400050002x
- Vannucci, S., D'Amato Avanzi, G., Galanti, Y., Gianecchini, R., Lo Presti, D., and Capilleri, P. P. (2019). Strength parameters of debris using a large shear box apparatus: application to a case history. *Rock Mech. Rock Eng.* 52, 4421–4437. doi:10.1007/s00603-019-01890-w
- Varotto, M., Bonardi, L., and Tarolli, P. (2019). *World terraced landscapes: history, environment, quality of life, environmental history*. Cham, Switzerland: Springer Nature Switzerland. doi:10.1007/978-3-319-96815-5
- Wei, W., Chen, D., Wang, L., Daryanto, S., Chen, L., Yu, Y., et al. (2016). Global synthesis of the classifications, distributions, benefits and issues of terracing. *Earth-Sci. Rev.* 159, 388–403. doi:10.1016/j.earscirev.2016.06.010
- Wooten, R. M., Gillon, K. A., Witt, A. C., Latham, R. S., Douglas, T. J., Bauer, J. B., et al. (2008). Geologic, geomorphic, and meteorological aspects of debris flows triggered by hurricanes Frances and Ivan during September 2004 in the southern Appalachian mountains of macon county, North Carolina (southeastern USA). *Landslides* 5 (1), 31–44. doi:10.1007/s10346-007-0109-9